

Argor Plasma Transport Properties

FACILITY FORM 602

N 66-12964 (ACCESSION NUMBER)	(THRU)
59 (PAGES)	1 (CODE)
CR-68297 (NASA CR OR TMX OR AD NUMBER)	25 (CATEGORY)

by
R. Stephen DeVoto

GPO PRICE \$ _____

CFSTI PRICE(S) \$ _____

Hard copy (HC) _____

Microfiche (MF) _____

653 July 65

February 1965

Report No. SU AA217*

Prepared under

National Aeronautics and Space Administration

Grant NsG 299-63

Submitted by **D. Bershader**

* This report was also issued as SUDAER No. 217 of the
Department of Aeronautics and Astronautics



**INSTITUTE FOR PLASMA RESEARCH
STANFORD UNIVERSITY, STANFORD, CALIFORNIA**

Sd/ 33582

ARGON PLASMA TRANSPORT PROPERTIES

by

R. Stephen DeVoto

February 1965

Reproduction in whole or in part
is permitted for any purpose of
the United States Government.

Report No. SU AA217*

Prepared under
National Aeronautics and Space Administration Grant NsG 299-63

Submitted by D. Bershader

*This report was also issued as SUDAER No. 217 of the
Department of Aeronautics and Astronautics

Institute for Plasma Research
Stanford University Stanford, California

ABSTRACT

12964

The transport properties of equilibrium argon plasma have been computed for pressures of 1, 10, 100, 760 and 1900 mm Hg and temperatures from 5000 to 20000°K. In addition to the usual viscosity and thermal conductivity, the thermal and multicomponent diffusion coefficients have also been computed. Two problems not occurring in computations of properties of un-ionized gases are examined. The first concerns the rate of convergence of the approximations to the transport coefficients. It is found that at least the third approximation to the thermal conductivity must be used down to very low degrees of ionization to ensure the accuracy of the results. Very slow convergence is also observed for the electron-atom, atom-electron and electron-ion diffusion coefficients at very low degrees of ionization. The source of this behavior is apparently the Ramsauer minimum in the electron-argon atom cross sections. The second problem occurs in the charged particle cross sections. In the present report the shielded Coulomb potential is used to bypass the divergence occurring in this cross section when the unshielded potential is used. Inclusion of terms of order unity in these cross sections increases the transport coefficients by appreciable amounts. Computations of electrical conductivity are also compared with some measured values here.

Author

TABLE OF CONTENTS

	<u>Page</u>
1. Introduction	1
2.1 Cross Sections for Argon	3
2.2 Equilibrium Transport Properties	17
2.3 Comparison of Electrical Conductivity with Experiment	36
3. Discussion and Conclusions	43
Appendix - Gas-Kinetic Cross Sections in Terms of Phase Shifts	48
Bibliography	51

LIST OF TABLES

<u>Table</u>	<u>Page</u>
1 The Electron-Atom Total Cross Sections $Q^{TOT}, Q^{(l)}$ (\AA^2) for $l = 1, 2, 3, 4$ vs Energy from Phase Shifts of Westin (1946)	12
2 Average Cross Sections $\bar{Q}^{(l,s)}$ (\AA^2) for Electron-Argon Atom Encounters	13
3 The Atom-Electron, Electron-Ion and Ion-Electron Diffusion Coefficients (cm^2/sec) for Equilibrium Argon at 1, 10, 100 and 1900 mm Hg	34

LIST OF ILLUSTRATIONS

<u>Figure</u>	<u>Page</u>
1. Average Atom-Atom, Atom-Ion and Electron-Atom Cross Sections $\bar{Q}^{(l,s)}$ for Argon	5
2. Electron-Argon Atom Gas-Kinetic Cross Sections $Q^{(l)}$ vs Electron Energy (eV), ($l = 1$)	8
3. Electron-Argon Atom Gas-Kinetic Cross Sections $Q^{(l)}$ vs Electron Energy (eV), ($l = 2$)	9
4. Electron-Argon Atom Gas-Kinetic Cross Sections $Q^{(l)}$ vs Electron Energy (eV), ($l = 3$)	10
5. Electron-Argon Atom Gas-Kinetic Cross Sections $Q^{(l)}$ vs Electron Energy (eV), ($l = 4$)	11
6. Average Electron-Argon Atom Cross Sections $\bar{Q}^{(l,s)}$ from 100 to 5000°K	14
7. Argon Charge-Transfer Cross Sections Q_{TR}^{TOT}	16
8. Average Argon Cross Sections $\bar{Q}^{(l,s)}$ for Ion-Atom Charge Transfer	18
9. Viscosity η of Equilibrium Argon at 1, 10, 100, 760 and 1900 mm Hg	21
10. Electrical Conductivity σ of Equilibrium Argon at 1 atm Showing Rate of Convergence of Approximations	22
11. Electrical Conductivity σ of Equilibrium Argon at 1, 10, 100 and 1900 mm Hg	23
12. Electrical Conductivity σ of Equilibrium Argon at 1 and 100 mm Hg Showing Effect of Higher Order Terms in Charged-Particle Cross Sections	24
13. Thermal Conductivity λ of Equilibrium Argon at 1 atm Showing Rate of Convergence of Approximations	25
14. Thermal Conductivity λ of Equilibrium Argon at 1, 10, 100 and 1900 mm Hg	26
15. Thermal Conductivity λ of Equilibrium Argon at 1 and 100 mm Hg Showing Effect of Higher Order Terms in Charged-Particle Cross Sections	27
16. Prandtl Number Pr of Equilibrium Argon at 1, 10, 100, 760 and 1900 mm Hg	29

<u>Figure</u>	<u>Page</u>
17. Thermal Diffusion Coefficients D_i^T of Equilibrium Argon at 1, 100 and 1900 mm Hg	30
18. Multicomponent Diffusion Coefficients D_{ij} of Equilibrium Argon at 1 atm	32
19. Electron-Ion D_{EI} and Atom-Electron D_{AE} Diffusion Coefficients of Equilibrium Argon at 1 atm Showing Rate of Convergence of Approximations	35
20. First Four Approximations to the Electron-Ion Diffusion Coefficients D_{EI} of Equilibrium Argon at 10 and 760 mm Hg for Temperatures from 2500 to 5500°K	37
21. Comparison of Predicted Argon Electrical Conductivity with Shock Tube Measurements at Initial Pressures of 1 mm Hg	39
22. Comparison of Predicted Argon Electrical Conductivity with Shock Tube Measurements at Initial Pressures of 10 mm Hg	40
23. Comparison of Predicted Argon Electrical Conductivity with Shock Tube Measurements at Initial Pressures of 100 mm Hg	41

1. Introduction

Computation of transport properties of ionized gases have in the past been carried out with either of two types of expressions: (1) the first or second approximation in the Chapman-Enskog method (Hirschfelder, Curtiss and Bird, 1964), (2) mixture rules, derived either as approximations to (1) (Brokaw, 1964) or with mean-free-path arguments (Fay, 1962; Lin et al, 1955). However, neither the theoretical expressions of (1) nor the usual mixture rules give correct values for the thermal conductivity in the limit of full ionization. This difficulty is bypassed with the mean-free-path relations by defining the electron-ion cross section in such a way that the properties take on the values derived by Spitzer and Härm (1953) when ionization is complete. However, this forced agreement in no way guarantees that the expressions will be accurate for other than very small and very high ionization. It is desirable to obtain theoretical expressions which automatically give the correct limiting values of the coefficients. This has been accomplished in an earlier report (de Voto, 1964; hereafter denoted by I).*

It is worthwhile to briefly summarize some important results of I. The theoretical expressions for thermal conductivity, thermal diffusion coefficient and multicomponent diffusion coefficient were extended to the fourth approximation and the viscosity to the second approximation. The formulation of Hirschfelder et al (1964) for these coefficients was generally followed. The expressions were then used in a study of the rate of convergence of the approximations to the transport coefficients for the fully ionized plasma (and also for several other simple binary mixtures). It was seen that at least the third approximation to the thermal conductivity and thermal diffusion coefficient must be used to obtain accurate coefficients for the plasma. The second approximations to the viscosity and electrical conductivity were adequate.

In this report the theoretical expressions are applied to the computation of properties of argon plasma. Argon was chosen for the calculations both because it is commonly used in plasma devices, and because a large

*The equation numbers of expressions taken from that report will be given with superscript I, e.g. (2.3)^I.

amount of information on the cross sections is available. This report has two aims in addition to a presentation of transport properties for use in analyzing flow situations. The first goal, which is evident from the remarks already made, is to investigate the rate of convergence of the approximations to the coefficients. The second includes a comparison of the transport coefficients as computed with and without the next higher order terms in the charged-particle cross sections. In the usual computations, all terms other than the dominant log terms are neglected. In I, an approximate method due to Liboff (1959), which uses the shielded potential for small angle deflections, was used to derive explicit expressions for the next higher order terms in these cross sections. These expressions enable one to compute properties more accurately than the cross sections derived with the usual Debye cutoff procedure.

The report has been divided into five sections: (1) the present introduction, (2) the computation of the cross sections, (3) the description of the results of the transport property calculations, (4) comparison of computed electrical conductivities with measurements, and (5) a final section in which the results are discussed. The expressions used for the computations will not be repeated here. Their general form is similar to those given in Chap. 7 of Hirschfelder et al (1964); complete details may be found in I.*

* An errata sheet for this report is appended.

2.1 Cross Sections for Argon

In partially ionized argon average cross sections must be determined for:

- (1) charged particles: e-e, e-A⁺, A-A⁺,
- (2) atom-atom: A-A,
- (3) electron-atom: e-A, and
- (4) atom-ion: A-A⁺.

Expressions for the average cross section $\bar{Q}^{(\ell,s)}$ for case (1) have been derived in I using the shielded Coulomb potential for small angle scattering (Liboff, 1959). They are

$$\bar{Q}^{(\ell,s)} = \frac{\alpha\pi(s-1)!}{(s+1)!} b_o^2 \left[\ell \ln \Lambda - \beta - 2\gamma + \sum_{n=1}^{s-1} \left(\frac{1}{n} \right) \right] \quad (3.12)^I$$

with $(\alpha,\beta) = (4, 1/2)$ for $\ell = 1$; $(12,1)$ for $\ell = 2$; $(12, 7/6)$ for $\ell = 3$; and $(16, 4/3)$ for $\ell = 4$. γ is Euler's constant (0.5772...), b_o is the average distance of closest approach $(Z_i Z_j e^2 / 2kT)$, and the plasma parameter Λ is defined differently depending on the relative size of the Debye length

$$d^2 = \frac{kT}{8\pi e^2 n_E} \quad (2.3)^I$$

and the interelectron distance, $h = n_E^{-1/3}$. Generally, $d > h$, but if $d < h$, as it is in equilibrium argon above about 400 mm Hg pressure, then $\Lambda = 2h/b_o$ will be used. Λ has been defined in such a way that neglect of the constant terms in (3.12)^I is equivalent to a cutoff of the $Q^{(\ell)}$ cross-section integrals at d (or h) and taking the average value of $(1/2)\mu g^2$ ($= 2kT$); see Chapman and Cowling, 1958, p. 179) in the argument of the logarithm.

For case (2), Amdur and Mason (1958) recommended that the potential

of interaction be taken as the repulsive exponential

$$\phi = \phi_0 \exp(-r/\rho) \quad (2.1)$$

For argon they give $\phi_0 = 3.23 \times 10^4$ eV and $\rho = 0.224\text{\AA}$. For this potential Monchick (1959) has already determined the average cross sections $\bar{Q}(\ell, s)$. He presents the results of his calculations as a table of $I(\ell, s)$ vs α , where

$$\bar{Q}(\ell, s) = \pi \sigma^2 \Omega(\ell, s)^* = \frac{16\pi(\ell+1) \alpha^2 \rho^2}{(s+1)! [2\ell - 1 - (-1)^\ell]} I(\ell, s) \quad (2.2)$$

and

$$\alpha = \ln(\phi_0/kT)$$

Unfortunately, Monchick only computed $I(\ell, s)$ for $\ell \leq 3$, so the computations here will be restricted to the third and lower approximation for most properties. In the actual computations it is necessary to interpolate between the values of the Table of Monchick. This was accomplished with Lagrange 3-point interpolation. Some of the cross sections so calculated are shown in Fig. 1.

For the electron-atom encounters it is preferable not to seek a classical potential as in the atom-atom case. The reason is that a non-classical phenomenon, namely the Ramsauer effect, occurs for this interaction, and it would probably be difficult to reproduce this effect with a simple classical potential. In argon the cross sections show a relative minimum at energies around .4 eV, and a maximum at several electron volts higher. This effect has been extensively studied, both with measurements of the total cross section given by

$$Q^{\text{TOT}}(g, \chi_0) = 2\pi \int_{\chi_0}^{\pi} \sigma(\chi, g) \sin \chi \, d\chi \quad (2.3)$$

and of the differential cross section $\sigma(\chi, g)$. The lower limit χ_0 is placed on the total cross section since the experiments always fail to detect scattering below a certain angle χ_0 . Unfortunately, almost all of the cross-section measurements are virtually useless

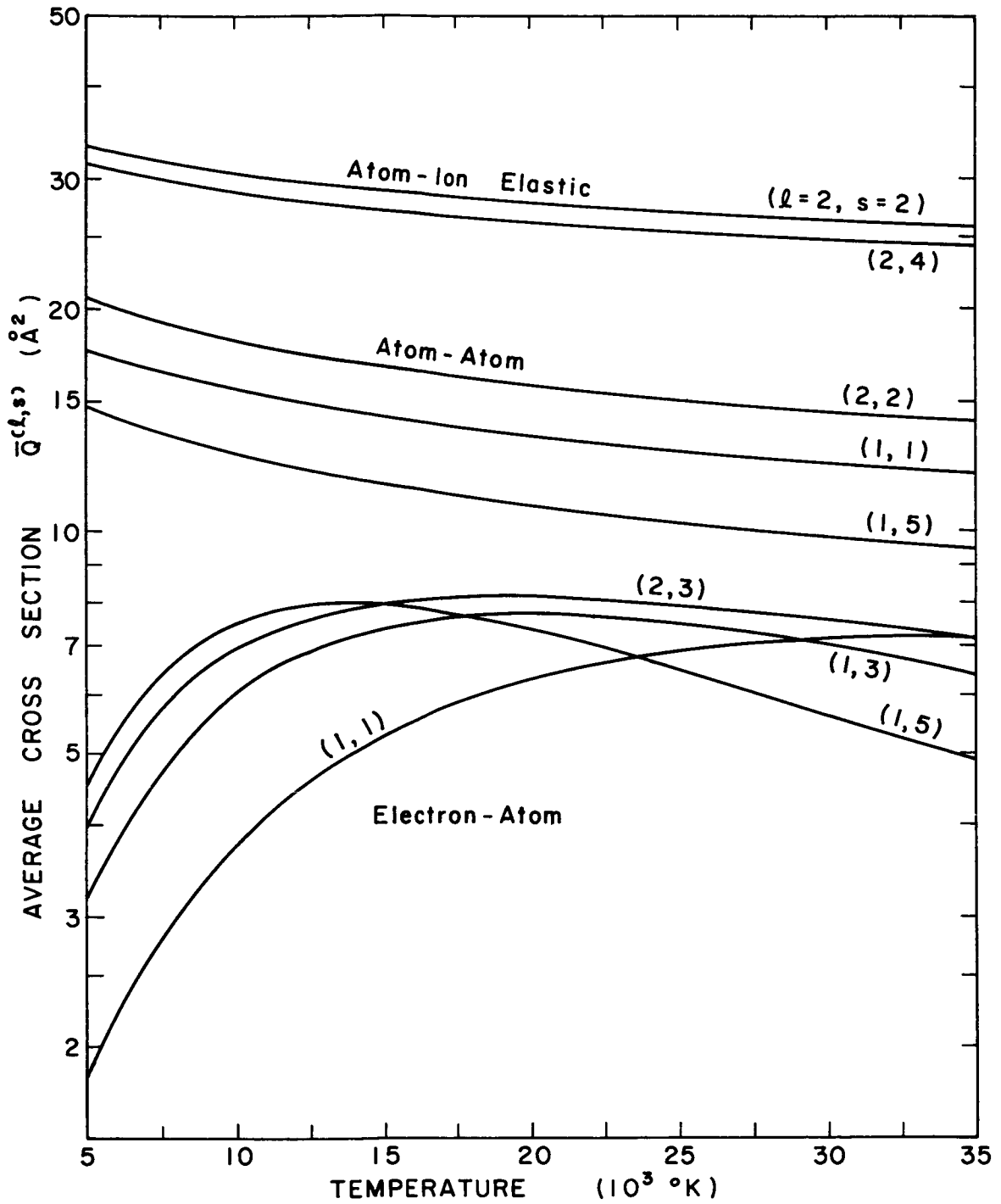


FIG. 1. AVERAGE ATOM-ATOM, ATOM-ION AND ELECTRON-ATOM CROSS SECTIONS $\bar{Q}^{(l,s)}$ FOR ARGON.

for determining the gas-kinetic cross sections (2.18)^I. The total cross sections cannot be used to determine $Q^{(\ell)}$ without a priori knowledge of the angular distribution of scattering. Additionally, most measurements fail to report the lower limit χ_0 on scattering angles detected.

In theory, the measurements of the differential cross section would furnish sufficient information to determine the $Q^{(\ell)}$. Most experimenters have evidently been unable to measure absolute values of $\sigma(\chi, g)$ and so report only relative values. A notable exception is given in the paper by Ramsauer and Kollath (1932). They report measurements of σ at 11 angles for electron scattering from argon at several relative energies from .6 to 12.5 eV. To determine the cross sections $Q^{(\ell)}$, their measured differential cross sections σ were fitted to a polynomial in χ , and this polynomial was used to compute the $Q^{(\ell)}$ integrand for use with Simpson's rule. It was possible to obtain a very good fit to the values obtained by Ramsauer and Kollath with a Stanford University program using orthogonal polynomials. The total cross sections ($\chi_0 = 0$) were calculated simultaneously with the $Q^{(\ell)}$ and compared with those measured by Ramsauer and Kollath (χ_0 unknown). Agreement was very good. The results for the gas-kinetic cross sections so calculated are shown in Figs. 2-5.

At energies below 0.6 eV, measurements of $\sigma(\chi, g)$ are not generally available. With the aid of effective range theory, O'Malley (1963) has recently analyzed some experimental measurements of Q^{TOT} , $Q^{(1)}$ and σ in the low-energy range to obtain formulas for the quantum-mechanical phase shifts η_ℓ . The gas-kinetic cross sections are given in terms of these phase shifts by (see Appendix)

$$Q^{(1)} = \frac{4\pi}{\kappa^2} \sum_{\ell=0}^{\infty} (\ell+1) \sin^2 (\eta_\ell - \eta_{\ell+1}) \quad (2.4a)$$

$$Q^{(2)} = \frac{4\pi}{\kappa^2} \sum_{\ell=0}^{\infty} \frac{(\ell+1)(\ell+2)}{(2\ell+3)} \sin^2 (\eta_\ell - \eta_{\ell+2}) \quad (2.4b)$$

$$\begin{aligned}
Q^{(3)} = \frac{4\pi}{\kappa^2} \sum_{l=0}^{\infty} & \left\{ \frac{(l+3)(l+2)(l+1)}{(2l+5)(2l+3)} \sin^2 (\eta_l - \eta_{l+3}) + \right. \\
& + (l+1) \left[\frac{(l+2)^2}{(2l+5)(2l+3)} + \frac{(l+1)^2}{(2l+3)(2l+1)} + \right. \\
& \left. \left. + \frac{l^2}{(2l+1)(2l-1)} \right] \sin^2 (\eta_l - \eta_{l+1}) \right\} \quad (2.4c)
\end{aligned}$$

$$\begin{aligned}
Q^{(4)} = \frac{4\pi}{\kappa^2} \sum_{l=0}^{\infty} & \left\{ \frac{(l+4)(l+3)(l+2)(l+1)}{(2l+7)(2l+5)(2l+3)} \sin^2 (\eta_l - \eta_{l+4}) + \right. \\
& + \frac{(l+2)(l+1)}{(2l+3)} \left[\frac{(l+3)^2}{(2l+7)(2l+5)} + \frac{(l+2)^2}{(2l+5)(2l+3)} + \right. \\
& \left. \left. + \frac{(l+1)^2}{(2l+3)(2l+1)} + \frac{l^2}{(2l+1)(2l-1)} \right] \sin^2 (\eta_l - \eta_{l+2}) \right\} \quad (2.4d)
\end{aligned}$$

In these equations, κ is related to the relative energy E by $E = 13.6a_0^2 \kappa^2$ with a_0 the Bohr radius. Cross sections calculated from the phase shifts determined by O'Malley are given in Figs. 2-5. Also shown are cross sections determined from calculations of the first two phase shifts η_0 and η_1 at four energies by Kivel (1959) (only these phase shifts are important at very low energies). We note that the cross sections of Kivel and O'Malley agree fairly well at the low energies. However, the curves determined from O'Malley's phase shifts diverge considerably at higher energies from the points calculated with the data of Ramsauer and Kollath. This behavior suggests that the effective range formulas used by O'Malley are applicable only at very low energies.

The last results to be used here have been obtained by Westin (1946). With the aid of a type of analog computer he obtained phase shifts from a large variety of experimental measurements, including his own. Cross sections computed from his phase shifts are given in Table I. From these results and the others mentioned above, "best fit" curves for $Q^{(l)}$, $l = 1-4$, were chosen. They are shown also

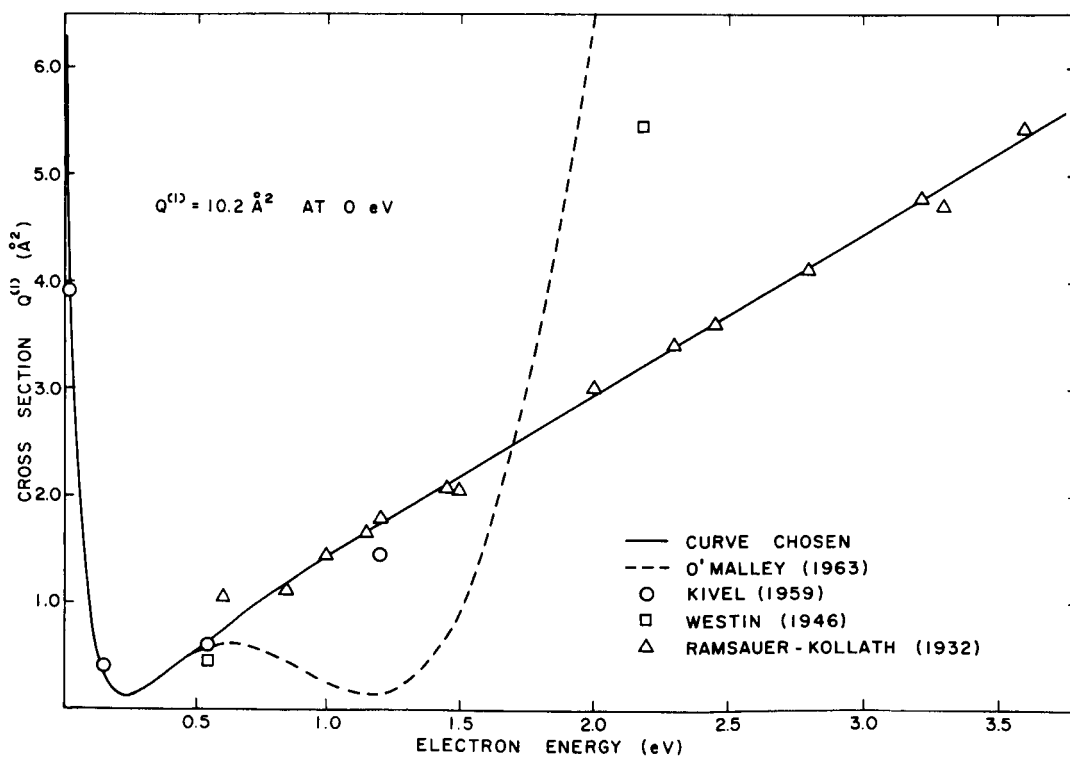
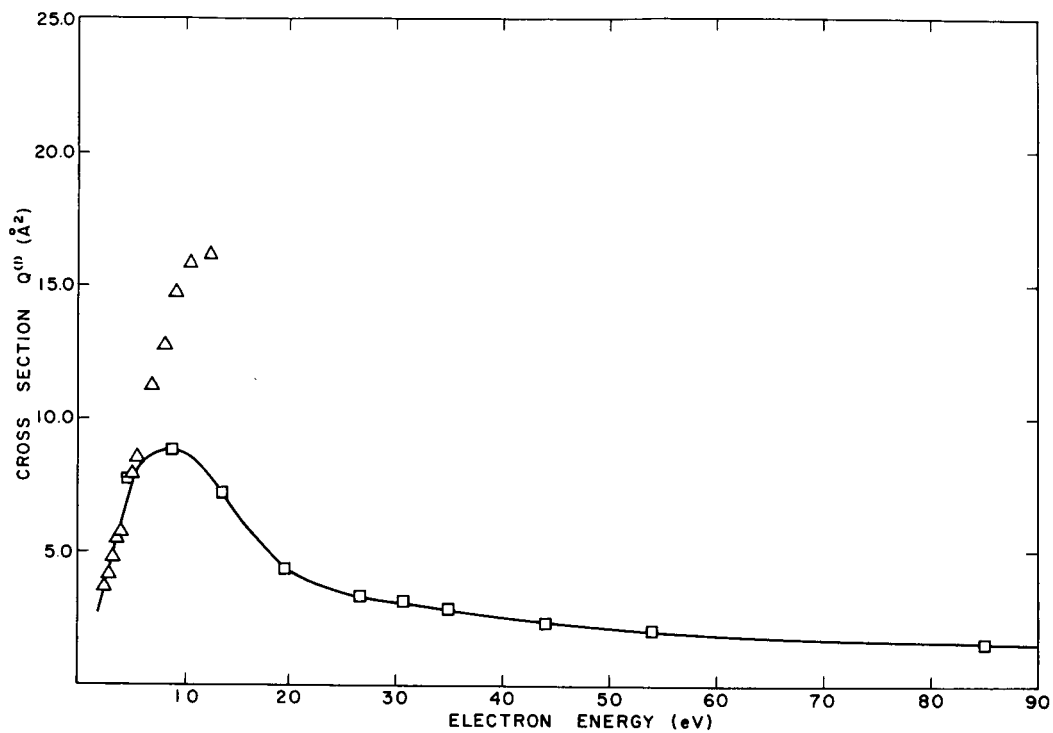


FIG. 2. ELECTRON-ARGON ATOM GAS-KINETIC CROSS SECTIONS $Q^{(l)}$ VS ELECTRON ENERGY (eV), ($l = 1$).

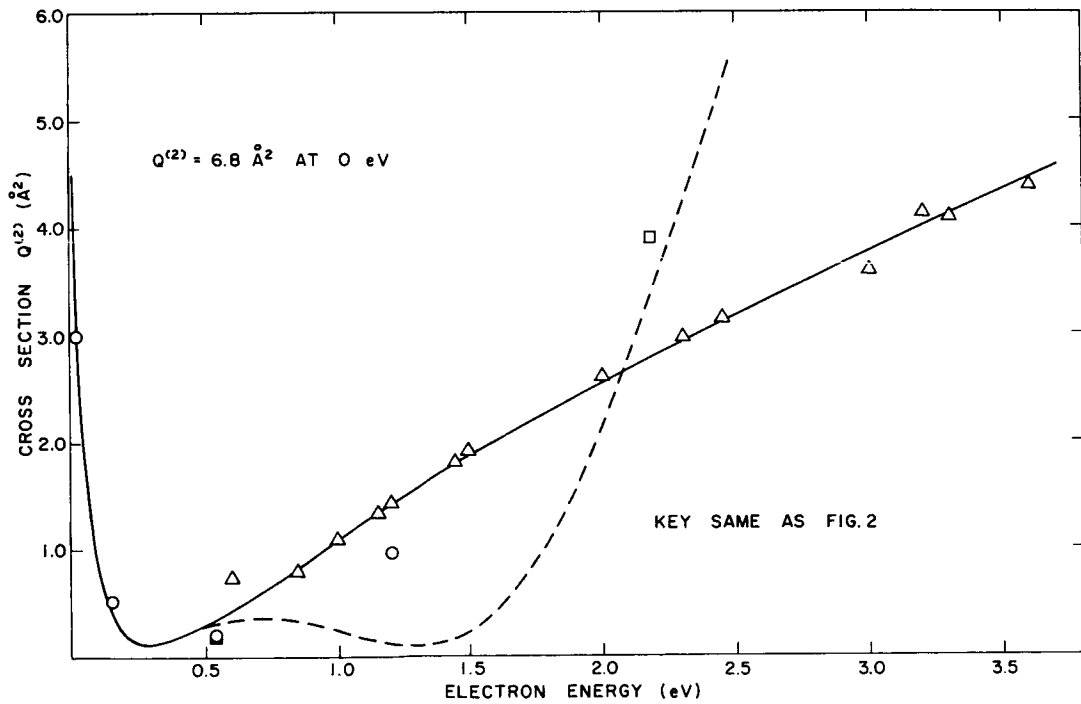
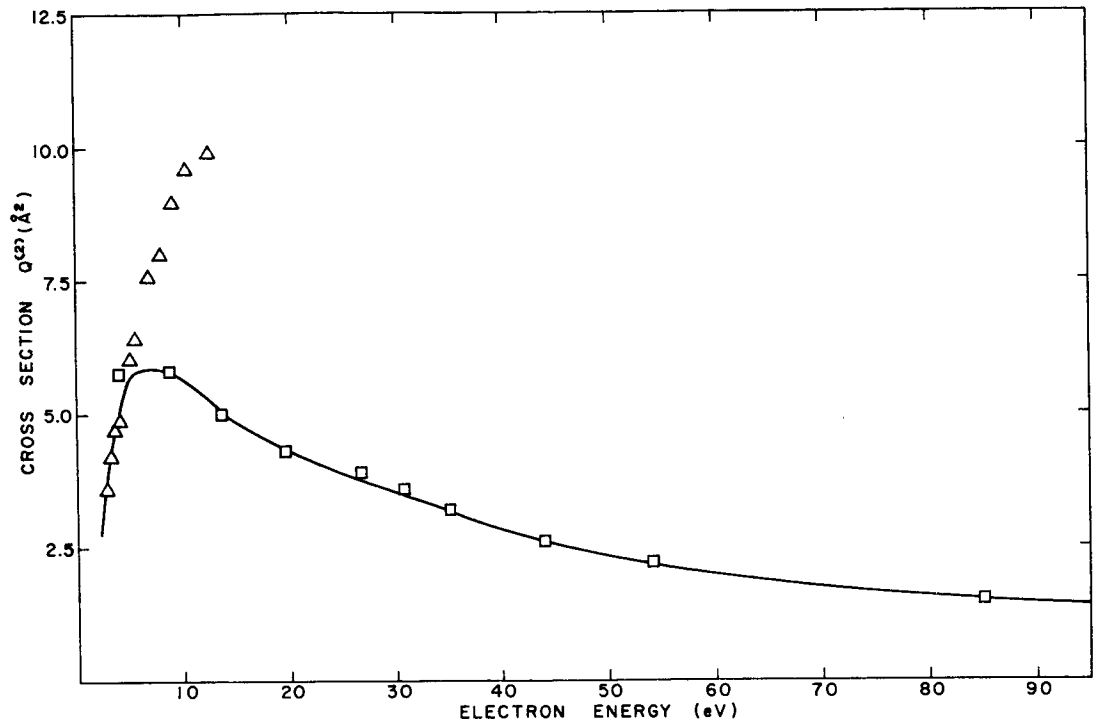


FIG. 3. ELECTRON-ARGON ATOM GAS-KINETIC CROSS SECTIONS $Q^{(l)}$ VS ELECTRON ENERGY (eV), ($l = 2$).

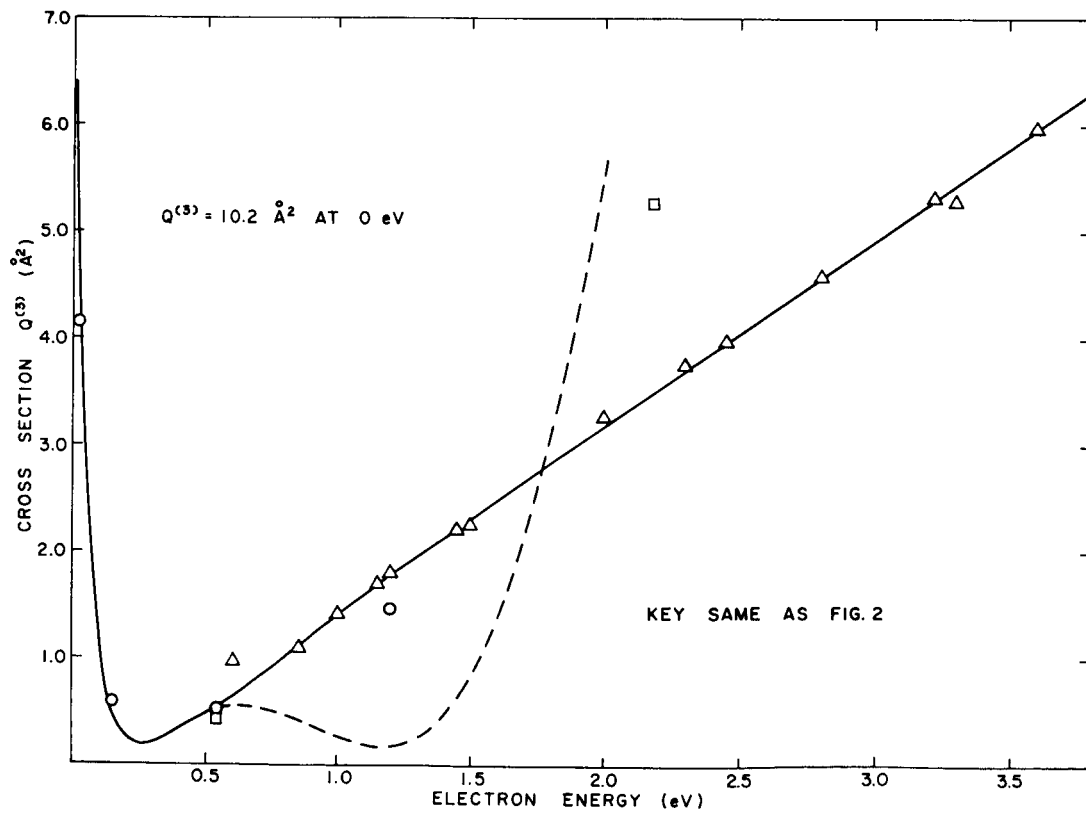
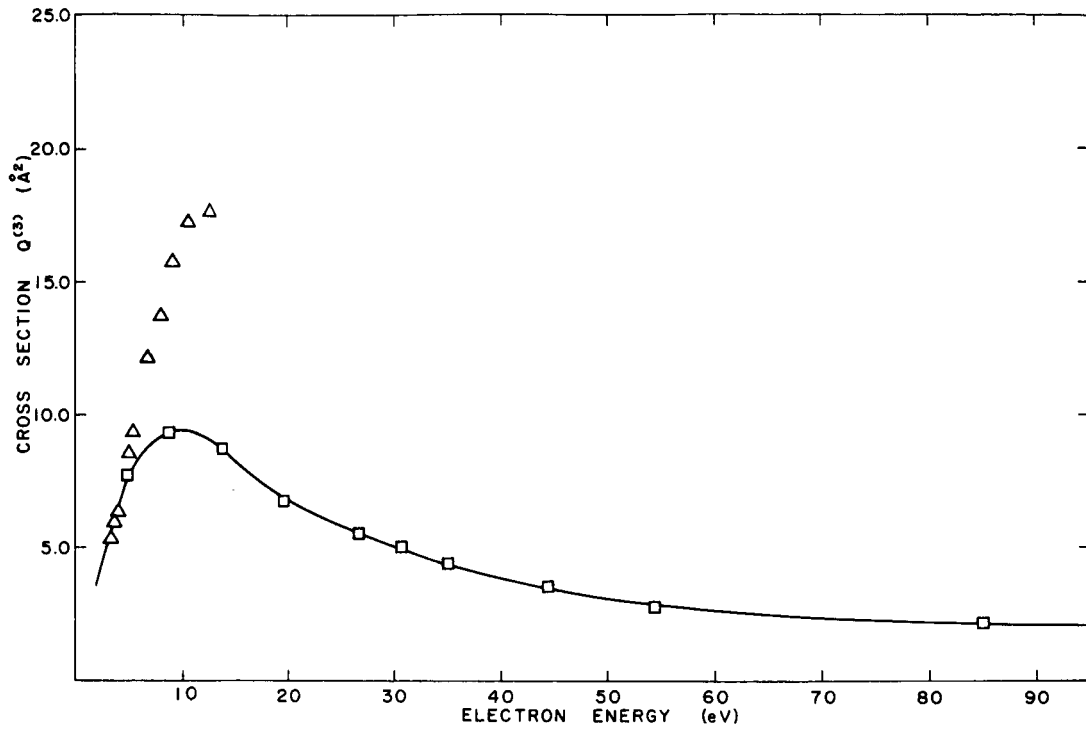


FIG. 4. ELECTRON-ARGON ATOM GAS-KINETIC CROSS SECTIONS $Q^{(l)}$ VS ELECTRON ENERGY (eV), ($l = 3$).

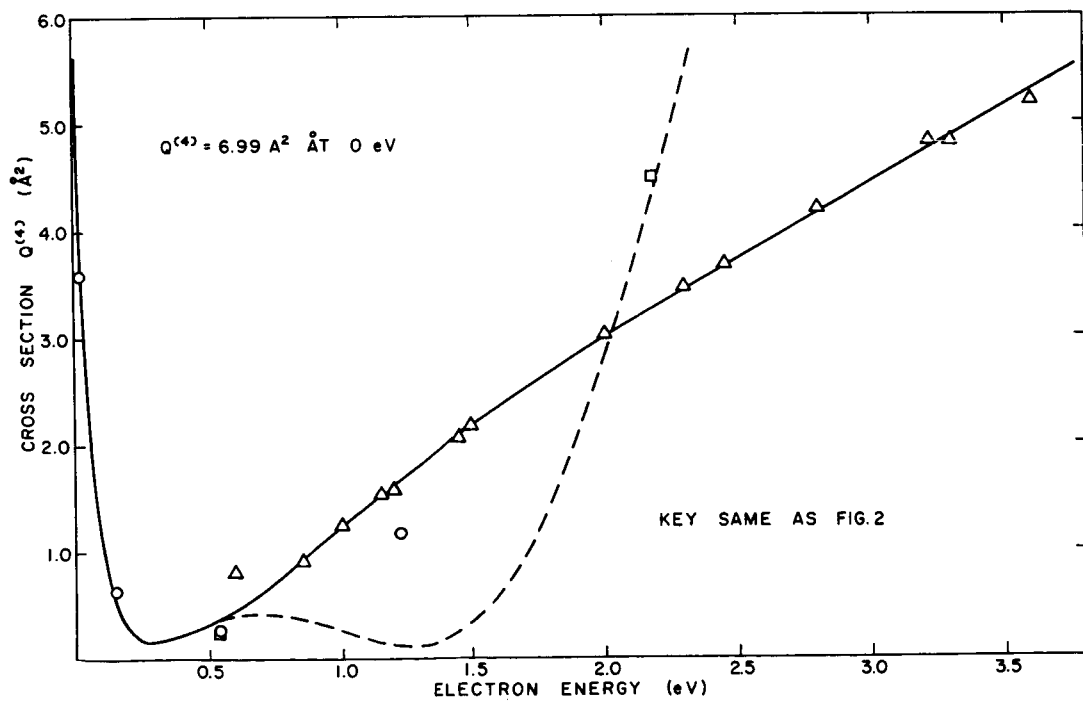
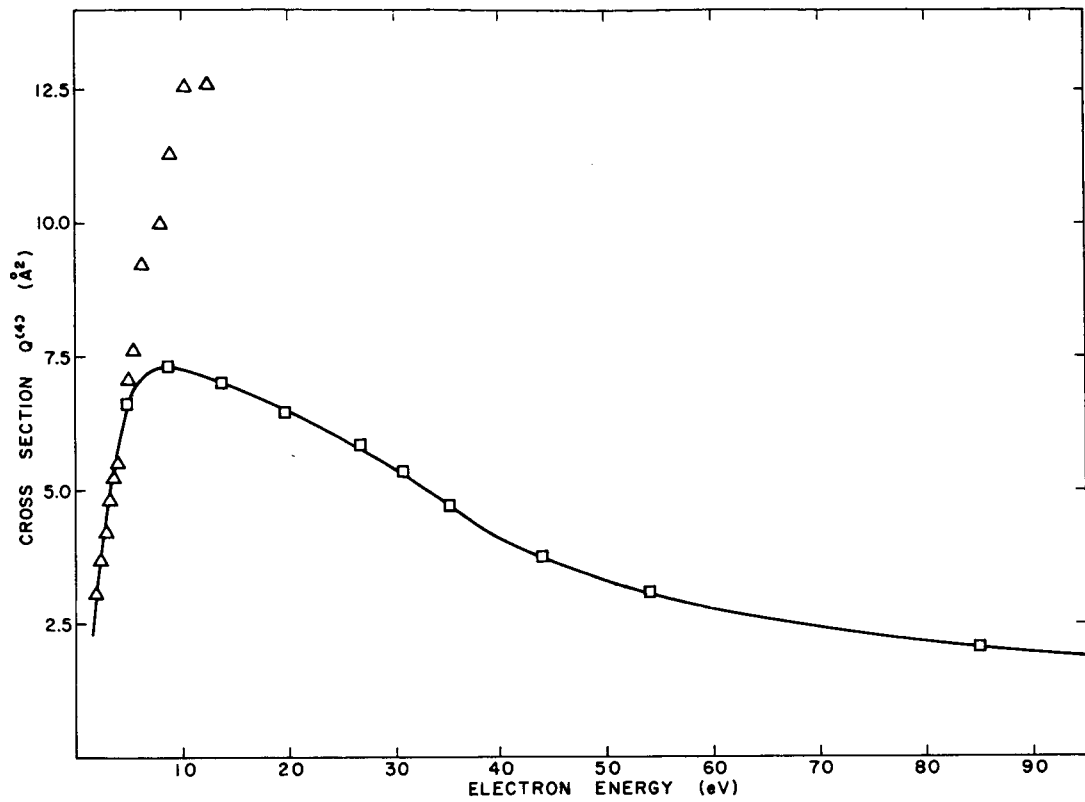


FIG. 5. ELECTRON-ARGON ATOM GAS-KINETIC CROSS SECTIONS $Q^{(l)}$ VS ELECTRON ENERGY (eV), ($l = 4$).

TABLE I. THE ELECTRON-ARGON ATOM TOTAL CROSS SECTIONS
 Q^{TOT} , $Q^{(\ell)}$, (\AA^2) FOR $\ell = 1-4$ VS ENERGY
 FROM PHASE SHIFTS OF WESTIN (1946)

Energy (eV)	Q^{TOT}	$Q^{(1)}$	$Q^{(2)}$	$Q^{(3)}$	$Q^{(4)}$
	(\AA^2)				
0.54	0.36	0.45	0.24	0.41	0.29
2.18	5.09	5.42	3.90	5.26	4.49
4.9	8.00	7.85	5.76	7.76	6.64
8.7	12.14	8.81	5.86	9.31	7.32
13.6	15.3	7.2	4.9	8.7	7.0
19.6	15.8	4.4	4.3	6.7	6.5
26.7	14.3	3.3	3.9	5.5	5.85
30.6	13.1	3.1	3.6	5.0	5.3
34.8	11.7	2.8	3.2	4.4	4.7
44.1	9.7	2.3	2.6	3.5	3.8
54.4	8.2	2.0	2.2	2.9	3.1
85.0	5.8	1.6	1.5	2.1	2.1
122.4	4.6	1.4	1.1	1.8	1.6

in Figs. 2-5. The cross sections from Westin's investigations were preferred to those of Ramsauer-Kollath above 5 eV because of his more extensive investigations at the higher energies.

Numerical integration with the aid of Simpson's rule was used to evaluate the average cross sections $\bar{Q}^{(\ell,s)}$ (2.17)^I. In this case the upper limit on the integrals was taken as $\gamma_0 = 110 \text{ eV/kT}$. The total range from 0 to γ_0 was divided into several smaller ranges, with the interval size in Simpson's rule determined by the rate of change of $Q^{(\ell)}$ with energy. Doubling the interval size changed the values of the integrals by less than 1%. Some of the average cross sections so computed are given in Table II and in Figs. 1 and 6. The Ramsauer minimum is clearly shown in Fig. 6, but occurs at different temperatures for different values of s because of the weighting factor $\exp(\gamma^2) \times \gamma^{2s+3}$ in the integrand of $\bar{Q}^{(\ell,s)}$.

TABLE II. AVERAGE CROSS SECTIONS $\bar{Q}^{(\ell,s)}$ (\AA^2) FOR ELECTRON-ARGON ATOM ENCOUNTERS

T(K)	(1,1)	(1,2)	(1,3)	(1,4)	(1,5)	(1,6)	(1,7)	(2,2)	(3,3)	(4,4)
100	4.29	3.55	2.98	2.53	2.15	1.83	1.57	4.09	3.25	3.11
200	2.74	2.01	1.50	1.12	0.84	0.63	0.48	2.51	1.73	1.59
300	1.90	1.25	0.83	0.57	0.40	0.30	0.24	1.67	1.03	0.91
400	1.38	0.83	0.52	0.35	0.27	0.25	0.26	1.17	0.67	0.58
500	1.04	0.59	0.38	0.29	0.28	0.31	0.36	0.86	0.49	0.43
600	0.82	0.47	0.33	0.30	0.34	0.40	0.48	0.66	0.41	0.37
700	0.68	0.40	0.33	0.35	0.42	0.51	0.61	0.54	0.38	0.37
800	0.58	0.38	0.36	0.42	0.51	0.62	0.74	0.47	0.39	0.41
900	0.52	0.38	0.40	0.49	0.61	0.74	0.86	0.44	0.42	0.47
1000	0.48	0.40	0.46	0.57	0.71	0.84	0.98	0.43	0.46	0.54
2000	0.63	0.85	1.12	1.40	1.69	1.98	2.26	0.91	1.13	1.59
3000	1.01	1.41	1.83	2.24	2.65	3.04	3.44	1.66	1.92	2.73
4000	1.41	1.96	2.51	3.04	3.57	4.10	4.62	2.42	2.69	3.76
5000	1.82	2.50	3.17	3.83	4.48	5.12	5.73	3.13	3.43	4.68
6000	2.23	3.03	3.82	4.59	5.33	6.02	6.63	3.80	4.13	5.49
7000	2.63	3.55	4.45	5.30	6.07	6.74	7.29	4.41	4.78	6.18
8000	3.02	4.05	5.03	5.91	6.67	7.28	7.74	4.97	5.36	6.75
9000	3.40	4.52	5.55	6.43	7.14	7.67	8.02	5.47	5.88	7.20
10000	3.77	4.96	6.01	6.86	7.49	7.92	8.16	5.91	6.34	7.57

For the ion-atom cross sections two types of processes must be considered. The first is the usual elastic collision and the second is that resulting from charge transfer between the atom and the ion. The latter process leads to a much higher cross section at lower energies, but Mason, Vanderslice and Yos (1959) have proved from scattering angle arguments that charge exchange does not affect the values of $Q^{(\ell)}$ for ℓ even. For ℓ odd they show that a good approximation is

$$Q^{(\ell)}|_{\ell \text{ odd}} = 2Q_{TR}^{TOT} \quad (2.5)$$

Two types of elastic interaction take place between the atom and the ion. The first is due to the polarization force and is of long range and attractive. The other force is short range and results from the mutual repulsion of the atomic fields. The latter dominates at the average energies of interest in this work, and will be the only force considered. Apparently the only determination of the short-range

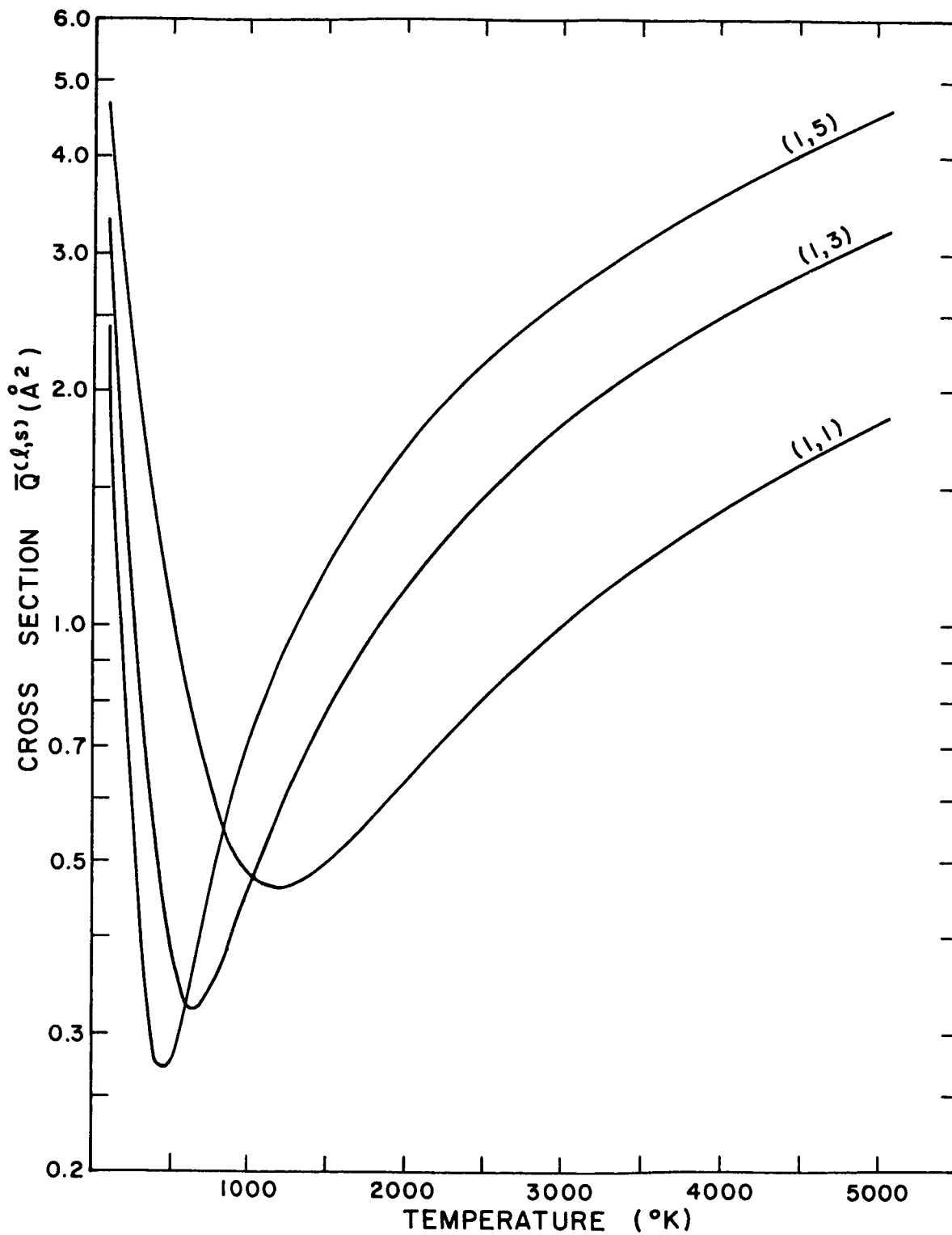


FIG. 6. AVERAGE ELECTRON-ARGON ATOM CROSS SECTIONS $\bar{Q}^{(l,s)}$ FROM 100 TO 5000 $^{\circ}\text{K}$.

force has been made by Cramer (1959) in ion scattering experiments. Cloney, Mason and Vanderslice (1962) have fitted his results with the exponential potential (5.1) and the constants $\phi_0 = 5.38 \times 10^6$ eV and $\rho = 1/5.08 \text{ \AA}$. Some calculations of the average cross sections made with this potential are given in Fig. 1.

Three types of information have been used to help determine the charge-transfer cross section: (1) ion beam scattering experiments, (2) ion mobility measurements, and (3) theory. Some results from the first source have been plotted in Fig. 7. All except one of the measurements lie above the energy range 0.5-2.0 eV that is most important for the present calculations. The ion mobility measurements have been made at temperatures of 100, 200 and 300° K. At the higher temperature, polarization forces are unimportant and the total cross section measured can be taken as due only to charge transfer. Dalgarno (1958) has examined a number of such measurements with the aid of theoretical formulas and adjusted certain constants to give a best fit to available data. From Fig. 7 we see that his final curve lies considerably above all scattering measurements except those of Gilbody and Hasted (1957). Apparently Dalgarno also considered these latter results in his analysis. Also shown are calculations from a theoretical formula due to Firsov (1951). The latter reproduce quite well the scattering results, but calculations not reproduced here show that they give average cross sections considerably below those determined from mobility measurements.

Dalgarno (1958) has also derived a relation based on theory which gives the general dependence of Q_{TR}^{TOT} on relative speed,

$$Q_{TR}^{TOT} = \frac{1}{2} (A - B \ln g)^2 \quad (2.6)$$

Two constants A and B are available in (5.6) and can be chosen to reproduce exactly the measured cross sections at two energies. Choosing to fit the measurements of Ziegler (1953) at 1 eV and those of Cramer (1959) at 50 eV, we obtain the constants

$$A = 25.61, \quad B = 1.196 \quad (2.7)$$

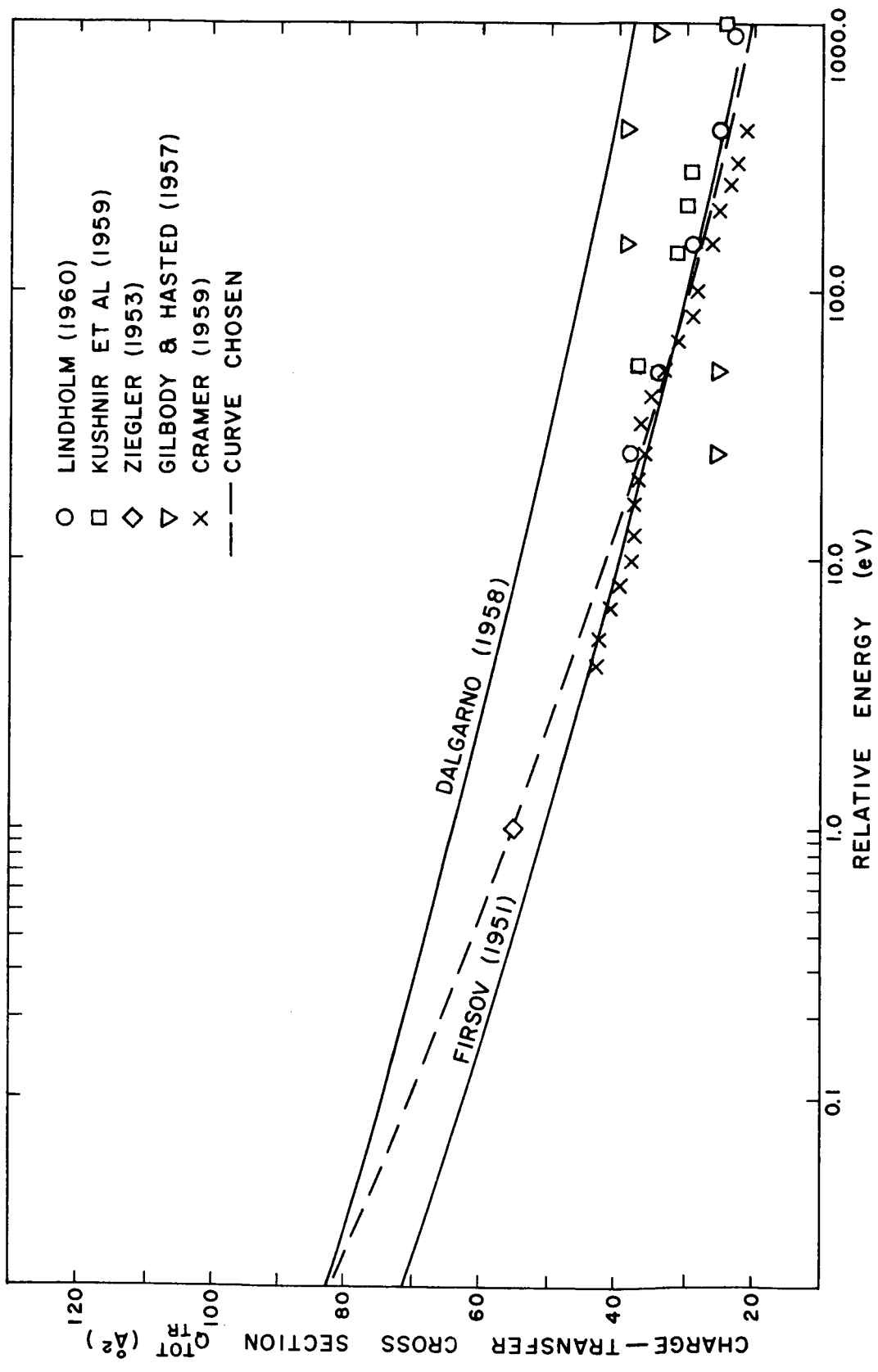


FIG. 7. ARGON CHARGE-TRANSFER CROSS SECTIONS Q_{TR}^{TOT} .

for Q_{TR}^{TOT} in \AA^2 . Computing the average cross sections with Simpson's rule, and using the relation

$$\mu_I = \frac{3e}{8n} \left(\frac{\pi}{m_I kT} \right)^{1/2} \frac{1}{\overline{Q}_{IA}^{(1,1)}} \quad (2.8)$$

we get an ion mobility of $1.62 \text{ cm}^2/\text{V-sec}$ at 300°K and $n = 2.69 \times 10^{19}/\text{cc}$. This compares very favorably with the measured value of 1.6 (Biondi and Chanin, 1957). In view of this agreement, and of the good agreement of this Q_{TR}^{TOT} with the beam measurements, it was decided to use the expressions (2.6), (2.7) and (2.5) with numerical integration to determine the average cross section $\overline{Q}^{(\ell,s)}$ for ℓ odd. Some results of the calculations are shown in Fig. 8.

5.2 Equilibrium Transport Properties

The calculations in this section will be restricted to singly ionized argon in thermodynamic equilibrium. The Saha equation has been used to determine the species composition. Defining the degree of ionization α by

$$\alpha = n_E / (n_E + n_A) \quad (2.9)$$

the equation takes the form

$$\alpha = \left[1 + \frac{h^3 p}{2(2\pi m_E)^{3/2}} \frac{Q_A}{Q_I} \frac{\exp(\theta/T)}{(kT)^{5/2}} \right]^{-1/2} \quad (2.10)$$

where θ is the ionization potential of the atom in $^\circ\text{K}$. The internal partition functions Q for the ions and atoms are given by the sum

$$Q = \sum_{n=1}^N g_n \exp\left(-\frac{\epsilon_n}{kT}\right) \quad (2.11)$$

where g_n is the degeneracy of the n th state whose energy is ϵ_n above the ground state of the atom or ion. The sum extends over all possible electronic states up to and including those with principal

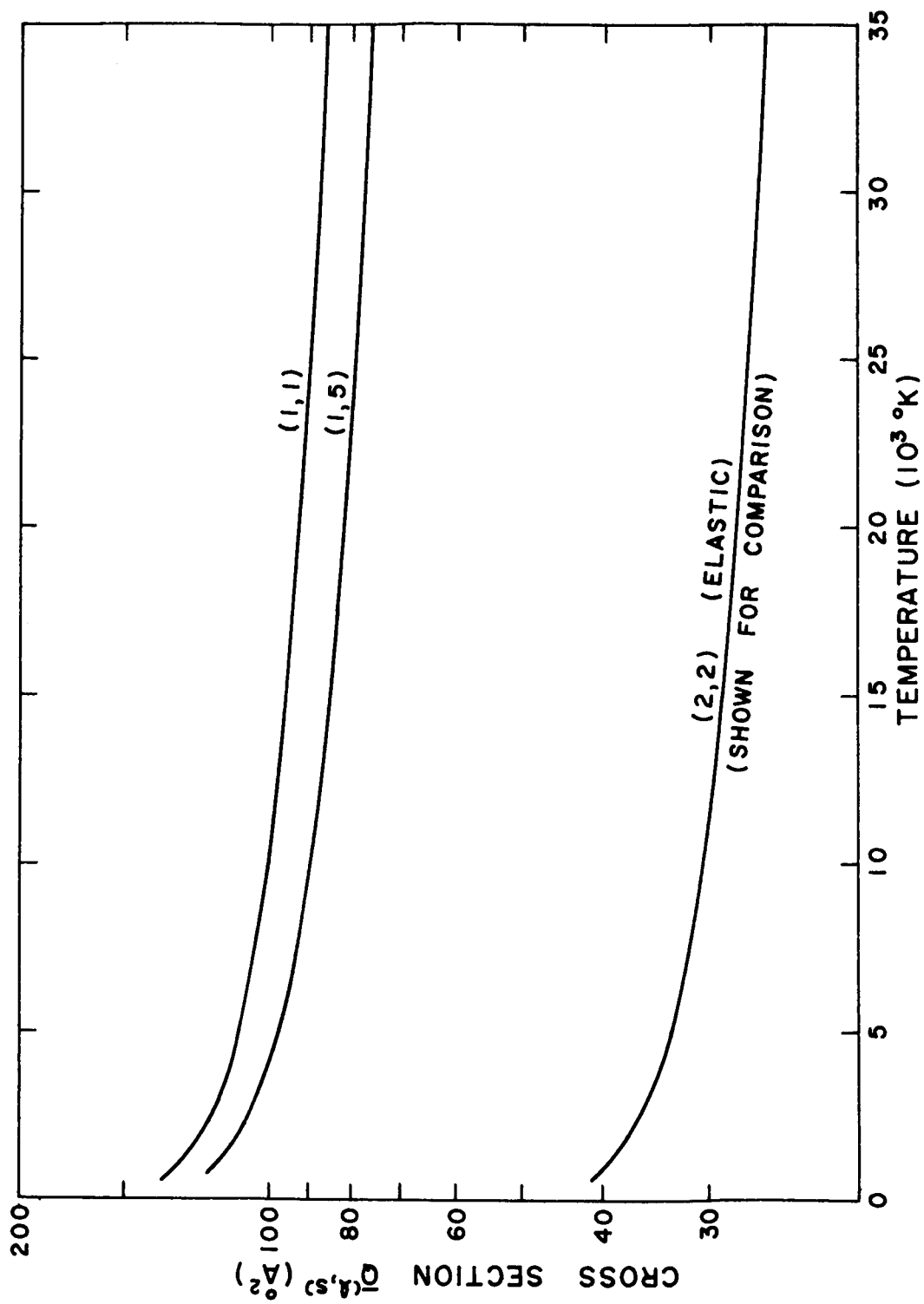


FIG. 8. AVERAGE ARGON CROSS SECTIONS $\bar{Q}^{(l,s)}$ FOR ION-ATOM CHARGE TRANSFER.

quantum number N . Following Drellishak, Knopp and Cambel (1963)*, N is determined by setting the Debye length d equal to the classical Bohr radius of the N th orbital,

$$N = \left(\frac{Z_{\text{eff}}}{a_0} \right)^{1/2} \left(\frac{kT}{8\pi e^2 n_E} \right)^{1/4} \quad (2.12)$$

with Z_{eff} the effective charge of the atomic or ionic core. Allowance is made for depression of the ionization potential by the amount

$$\Delta\theta = \frac{\theta}{N^2} \quad (2.13)$$

Since the electron number density occurs in the criterion for the cutoff of the partition function sums (2.11), it is necessary to use an iterative process to determine the composition. The values of N for the atom and ion were first guessed and the composition was calculated with (2.10), (2.12), and (2.13). The new values of N were used repeatedly as guesses until agreement was attained between initial and computed values. The number densities so calculated agree closely with those of Drellishak et al, and will not be given here.

The general computer program mentioned earlier was used for the property calculations. The calculations of most properties were performed for temperatures from 5000-20000°K and for pressures of 1, 10, 100, 760 and 1900 mm Hg. The upper limit on temperature represents approximately the point where the second ion becomes important; below the lower limit all properties except diffusion coefficients can be computed neglecting the ionization (Amdur and Mason, 1958). At the two higher pressures (1 and 2-1/2 atm), it was found that the Debye length was shorter than the interelectron distance. At these pressures the charged-particle cross sections were computed with a cutoff at the interelectron distance and the higher order terms neglected. At the lower pressures the complete expressions as listed in Eq.(3.12)^I were used.

* These authors kindly furnished copies of their program decks from which the energy levels used in the present work were taken.

The viscosity is plotted in Fig. 9. Where not otherwise indicated, the curves are for the second approximation. As might be expected from the results of I (Tables 3 & 11), the difference between the first and second approximations to this coefficient is important only at higher degrees of ionization. The large decrease in viscosity is due, of course, to the very large charged-particle cross section which determines the ion contribution. In Fig. 9 are also shown results of the second approximation at 100 mm in which the higher order terms in the charged-particle cross section are neglected. It appears that the inclusion of these higher order terms has a greater effect on the viscosity than does the increase in level of approximation.

The electrical conductivity, as computed from the electron-ion diffusion coefficient D_{EI} with the aid of (2.26a)^I, is shown in Figs. 10-12. In the first figure we see that the first approximation is poorest at high degrees of ionization, but becomes better around 8000°K for 1 atm pressure. Since the electrical conductivity is proportional to the number density of the electrons, it decreases rapidly below this temperature and will not be shown. It may be calculated quite readily down to 2500°K from the electron-ion diffusion coefficients to be presented later. It will turn out that at least the third and preferably the fourth approximation to D_{EI} and hence to σ must be used for equilibrium argon below about 5000°K. In the curves of Fig. 12, we see that the higher order terms in the charged-particle cross section also have considerable effect on the electrical conductivity.

In Fig. 13, where the thermal conductivity for argon at 1 atm is plotted, we see one of the most pronounced effects of the use of higher approximations. The third approximation rises above the first and second at less than 0.5% ionization. The difference increases until at $\alpha = 0.58$ ($T = 15000^{\circ}\text{K}$) and higher, the third approximation is more than two times the lower approximations. It is apparent that any approximate formula for the thermal conductivity of a partially ionized gas which is based solely on the second approximation will be seriously in error. We also see in Figs. 13 and 15 that the expression of

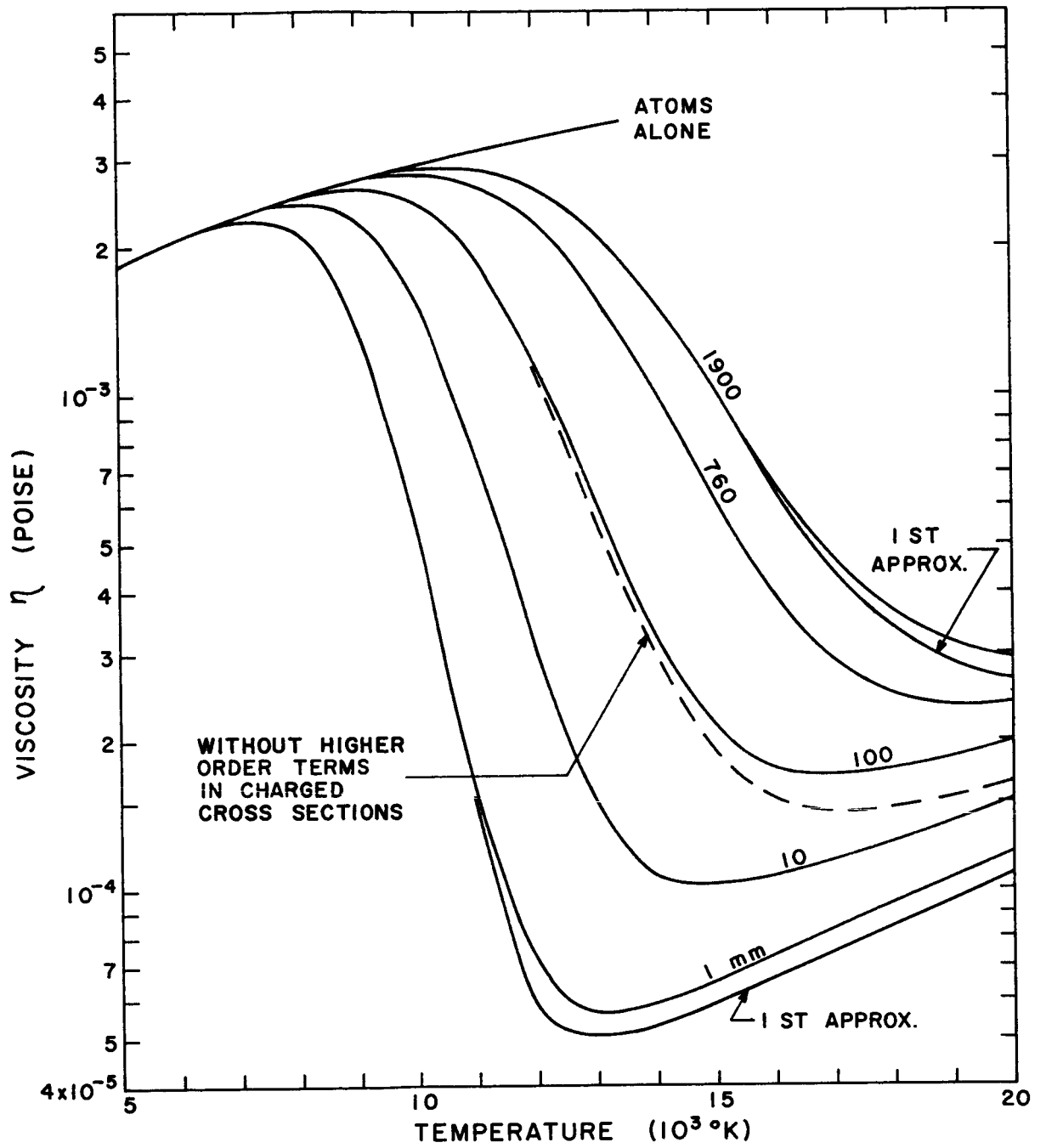


FIG. 9. VISCOSITY η OF EQUILIBRIUM ARGON AT 1, 10, 100, 760 and 1900 mm Hg.

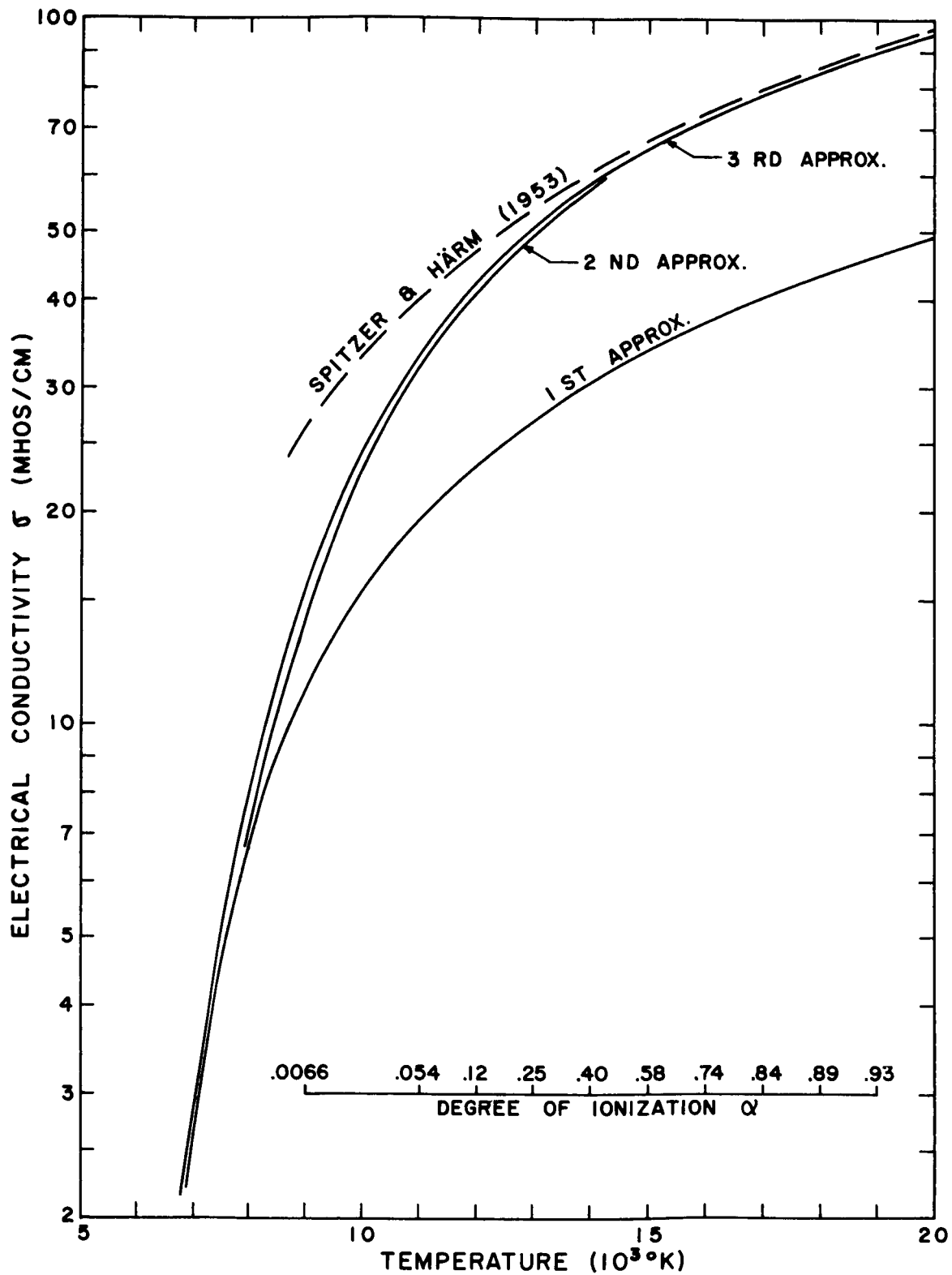


FIG. 10. ELECTRICAL CONDUCTIVITY σ OF EQUILIBRIUM ARGON AT 1 ATM SHOWING RATE OF CONVERGENCE OF APPROXIMATIONS.

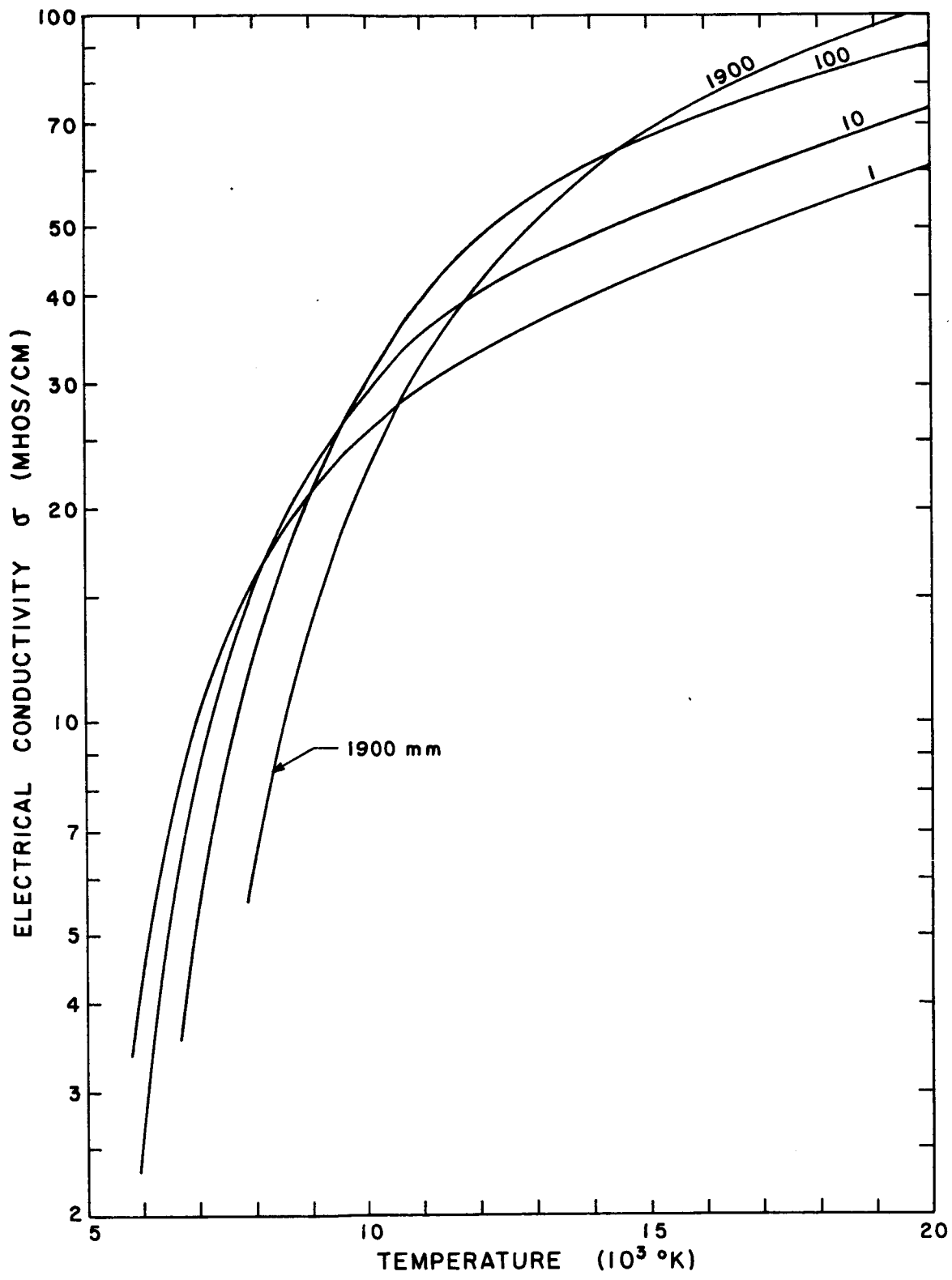


FIG. 11. ELECTRICAL CONDUCTIVITY σ OF EQUILIBRIUM ARGON AT 1, 10, 100 and 1900 mm Hg.

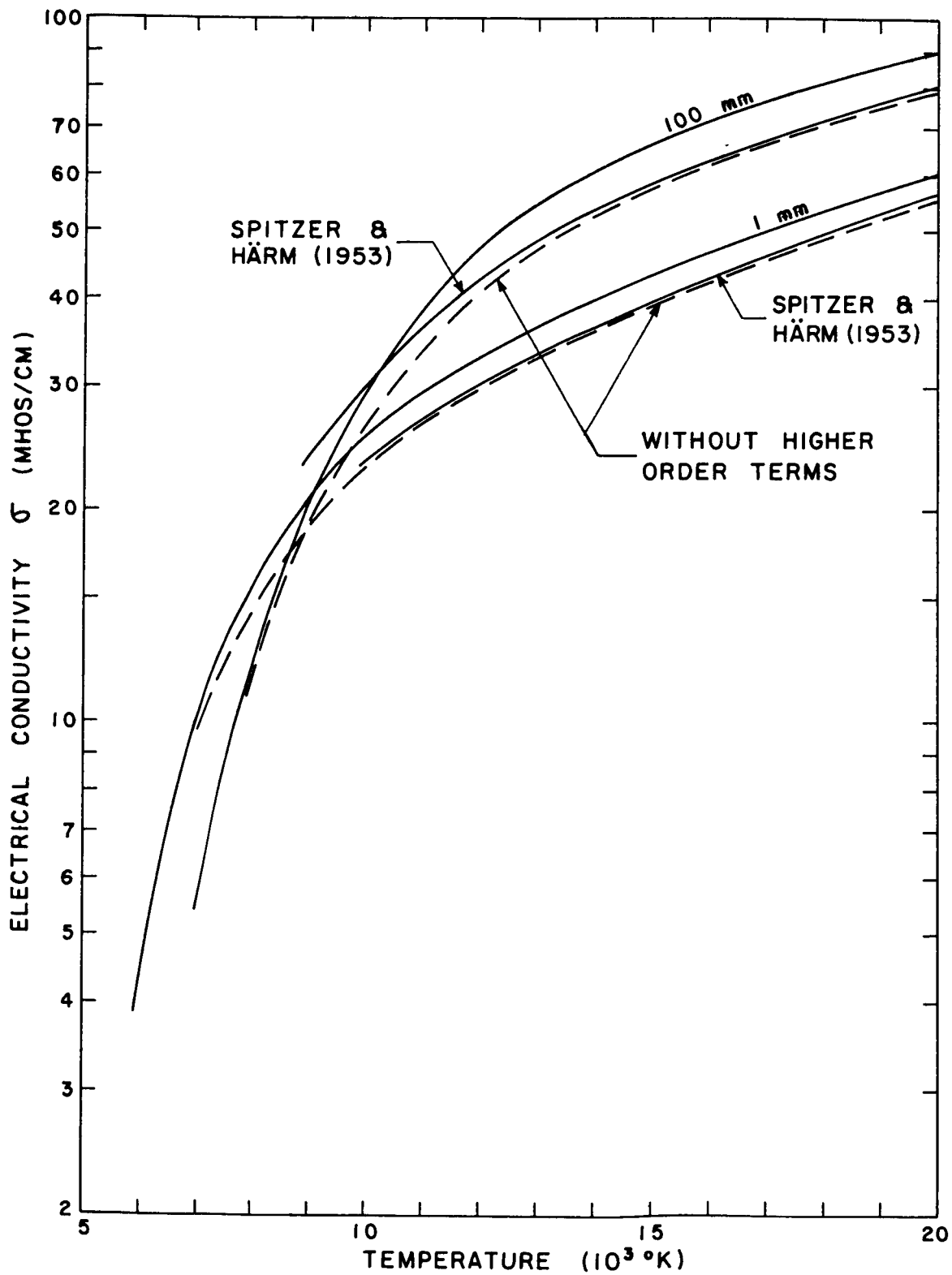


FIG. 12. ELECTRICAL CONDUCTIVITY σ OF EQUILIBRIUM ARGON AT 1 AND 100 mm Hg SHOWING EFFECT OF HIGHER ORDER TERMS IN CHARGED-PARTICLE CROSS SECTIONS.

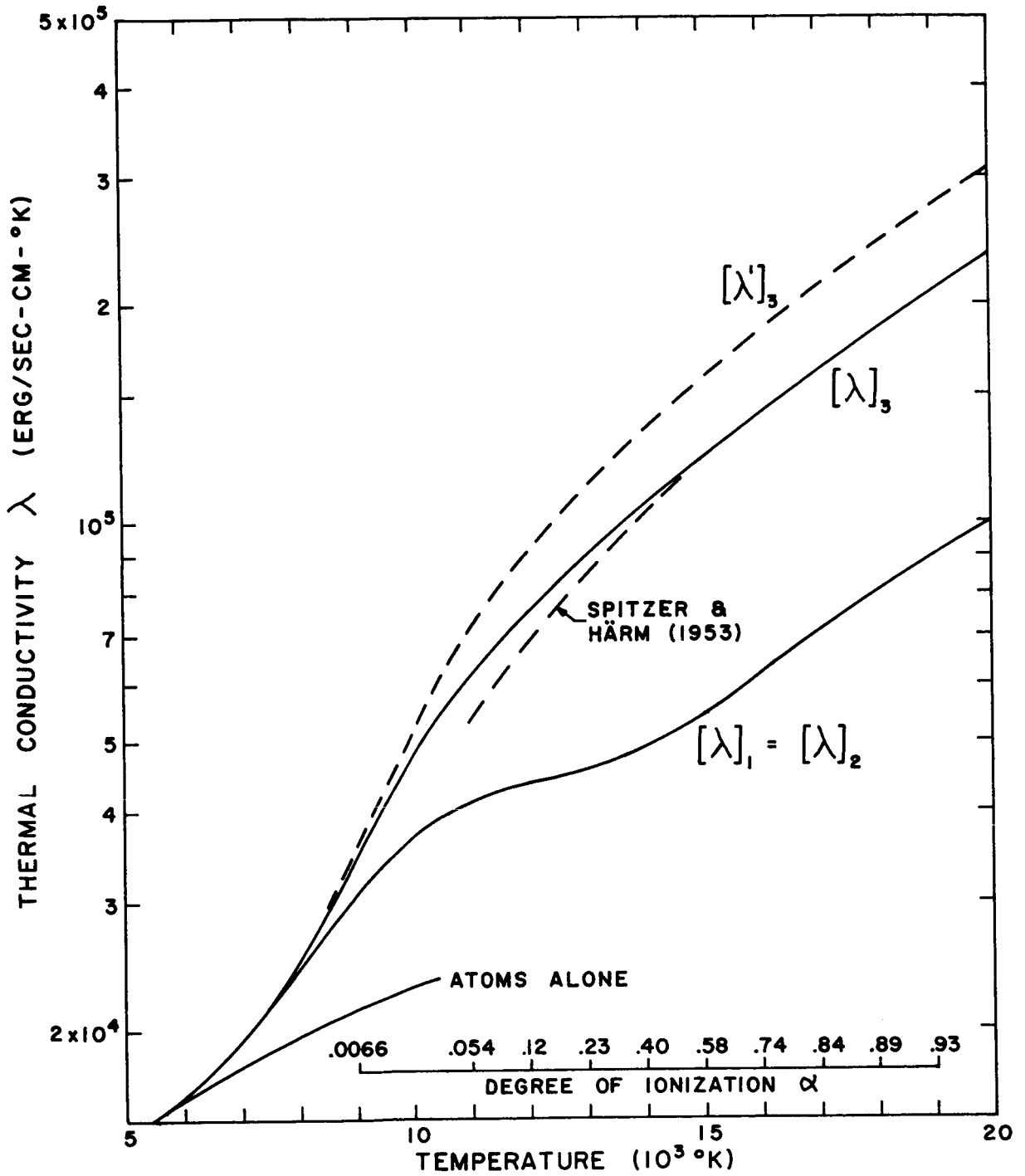


FIG. 13. THERMAL CONDUCTIVITY λ OF EQUILIBRIUM ARGON AT 1 ATM SHOWING RATE OF CONVERGENCE OF APPROXIMATIONS.

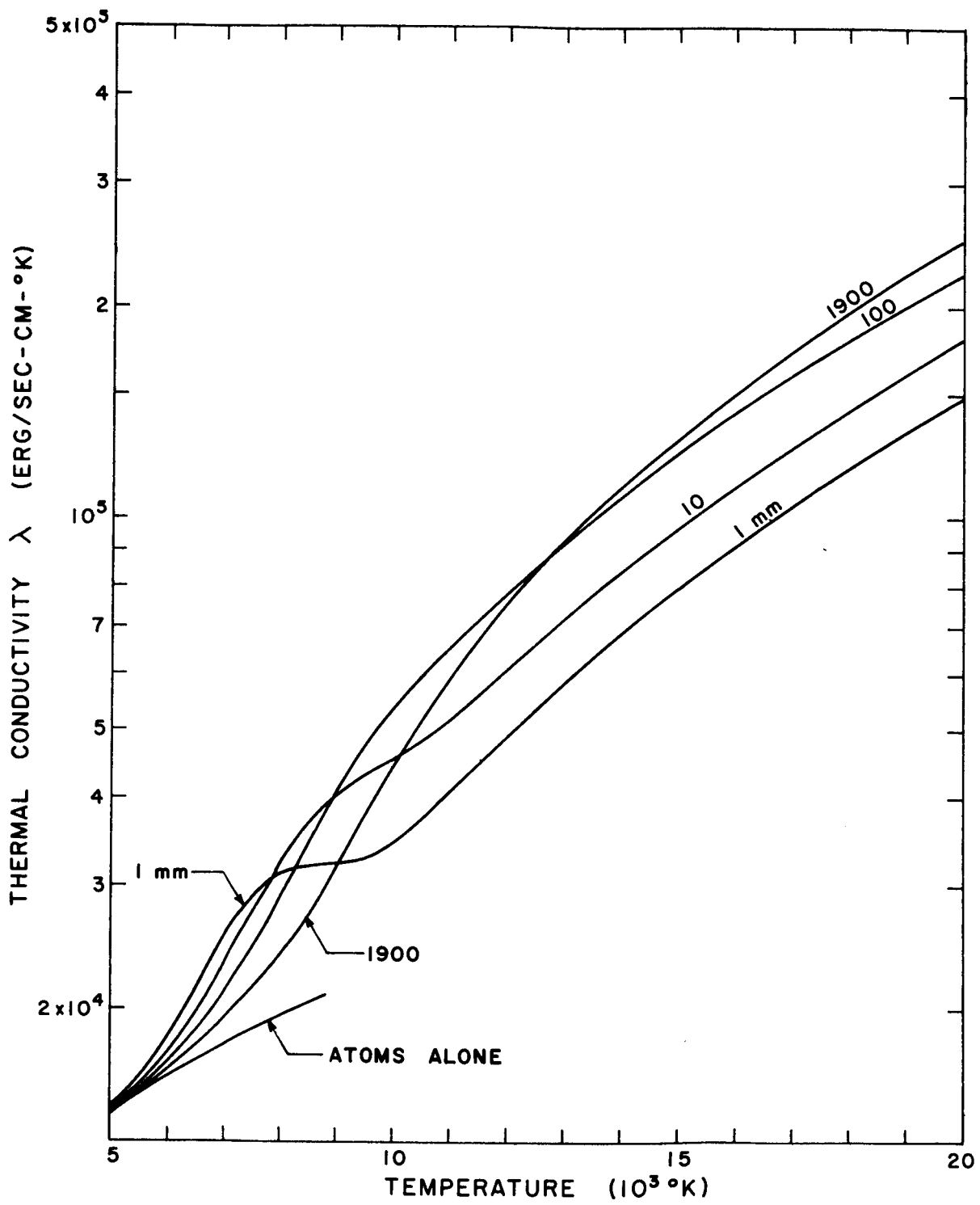


FIG. 14. THERMAL CONDUCTIVITY λ OF EQUILIBRIUM ARGON AT 1, 10, 100 and 1900 mm Hg.

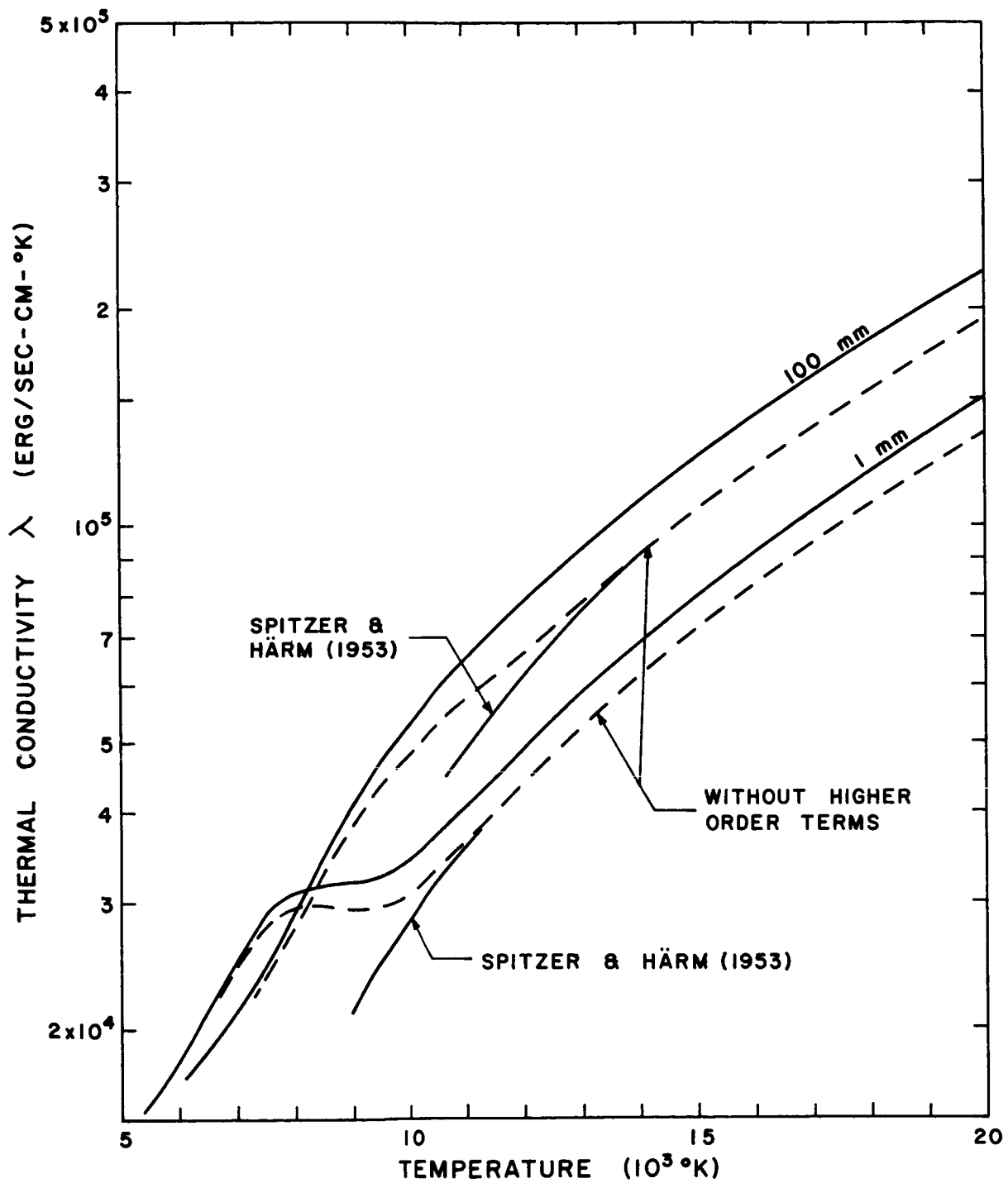


FIG. 15. THERMAL CONDUCTIVITY λ OF EQUILIBRIUM ARGON AT 1 AND 100 mm Hg SHOWING EFFECT OF HIGHER ORDER TERMS IN CHARGED-PARTICLE CROSS SECTIONS.

Spitzer and Härm (1953) gives results very close to the third approximation as computed without higher order terms in the charged cross sections. At lower degrees of ionization the formula of Spitzer and Härm underestimates the thermal conductivity by about 20% for a pressure of 1 atm. In this region the electron-atom collisions, for which the average cross section is quite small, become more important and hence allow freer conduction by the electrons. This effect shows up more prominently as inflection points in the thermal conductivity curves at 1 and 10 mm pressure (Fig. 14).

The results in Figs. 9, 13-14 have been combined to yield values for the Prandtl number shown in Fig. 16. For singly ionized argon, this quantity is given by

$$\text{Pr} = (5/2)(1 + \alpha)(k\eta/\lambda m_A) \quad (2.14)$$

The large increase in λ and decrease in η with increasing ionization causes Pr to fall to very low values.

Figure 17 shows values of third approximations to the diffusion coefficients. For the electrons, this coefficient D_E^T is much smaller than those for the atom and ion over most of the low-temperature range considered. So, from

$$\sum_{i=1}^v D_i^T = 0$$

we have $D_I^T \sim -D_A^T$. However, at high degrees of ionization, only the ions and electrons are important, so $D_I^T = -D_E^T$. Since $D_A^T < 0$ and $D_E^T > 0$, D_I^T must pass through zero at some point where, necessarily, $D_A^T = -D_E^T$. We see from Fig. 17 that this occurs around 17400°K for $p = 1$ mm and above 20000°K for the higher pressures.

The difference between the second and third approximations to the thermal diffusion coefficients will not be shown here (this coefficient is zero in the first approximation). As might be expected from the studies of I (Sec 3), the rate of convergence of this coefficient was found to be quite slow. For example, at 6000°K and 1 atm, D_I^T increased by 338% from the second to the third approximation. The

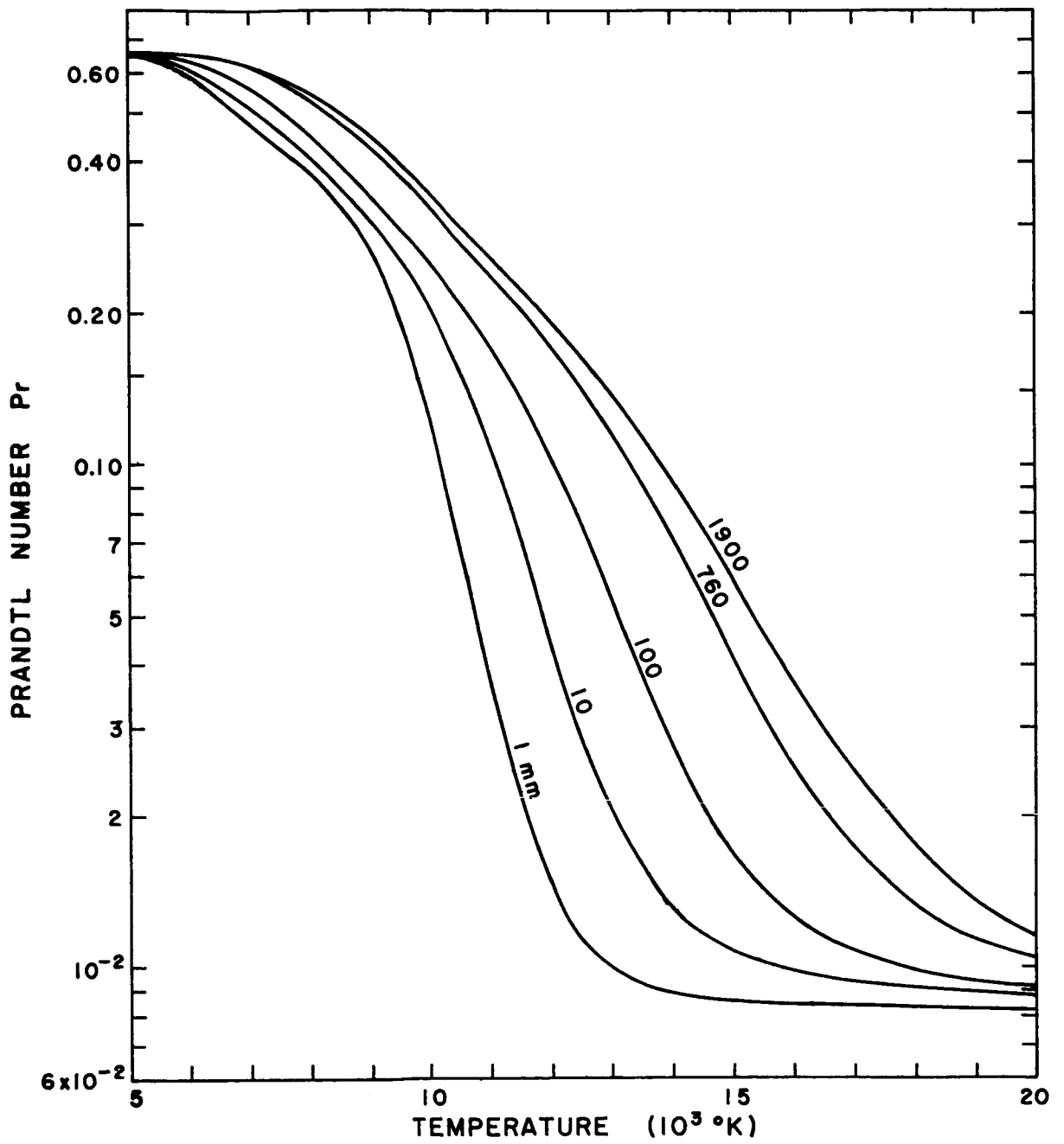


FIG. 16. PRANDTL NUMBER Pr OF EQUILIBRIUM ARGON AT 1, 10, 100, 760 AND 1900 mm Hg.

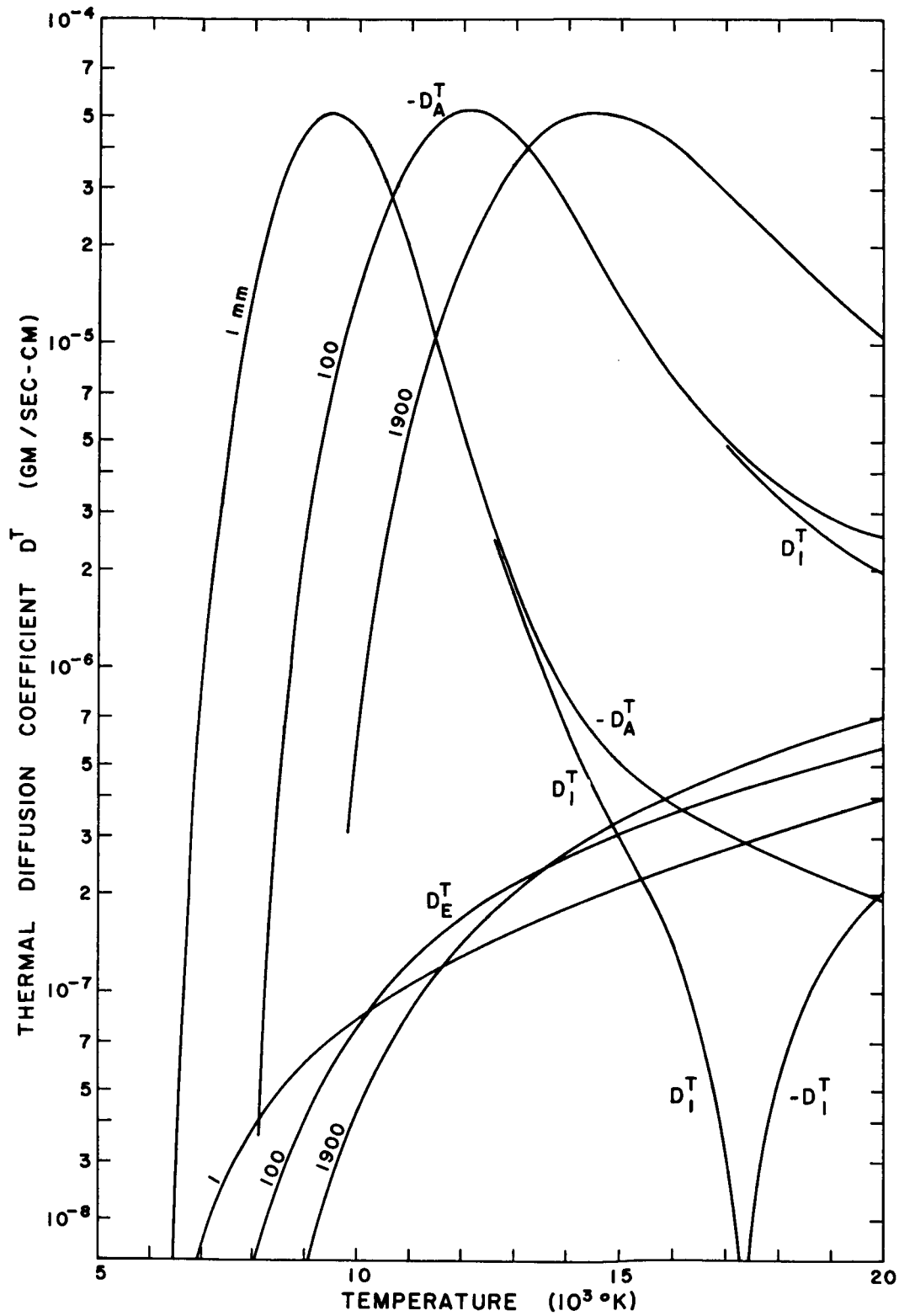


FIG. 17. THERMAL DIFFUSION COEFFICIENTS D_i^T OF EQUILIBRIUM ARGON AT 1, 100 and 1900 mm Hg.

fourth approximation was also calculated for these conditions, with the use of the approximate cross sections in (2.18), and was higher than $[D_I^T]_2$, by 425%. The example just cited was an extreme case, and at higher temperatures the change from the second to the third approximation was considerably less. For example, at 15000°K and 1 atm, with a degree of ionization of 58%, the change was -12, 2.2 and -2.2%, respectively, for the electron, ion and atom coefficients.

The third approximations to all of the multicomponent diffusion coefficients for $5000\text{--}20000^\circ\text{K}$ and 1 atm pressure are plotted in Fig. 18. Because of the very large charge-transfer cross section and the higher masses, the ion-atom and atom-ion diffusion coefficients lie considerably below the others. It turns out to be a very good approximation to take $D_{IA} = D_{AI} = [D_{IA}]_1$, where the latter is the binary coefficient and is found from

$$[D_{ij}]_1 = \frac{3}{16n} \left(\frac{m_i + m_j}{m_i m_j} \right)^{1/2} \frac{(2\pi kT)^{1/2}}{\bar{Q}_{ij}(1,1)} \quad (2.15)$$

Actually, this relation follows from the expression (HCB, p. 716),

$$D_{12} = D_{12} \left[1 + \frac{n_3(m_3 D_{13}/m_2 - D_{12})}{n_1 D_{23} + n_2 D_{13} + n_3 D_{12}} \right] \quad (2.16)$$

which holds in the first approximation, when we consider the order in electron mass of each term for D_{IA} and D_{AI} . The very rapid convergence might be expected from the hard-sphere nature of the average ion-atom cross sections (Figs. 1, 8) for which the convergence of diffusion coefficients is quite rapid.

No similar simplifications, either regarding the rate of convergence or the relation between the multi and binary coefficients, were found for the other pairs of species. It is evident from (2.16) that the multicomponent diffusion coefficients are not symmetric when the electron is involved. It is evident also from (2.16) that, at least in the first approximation,

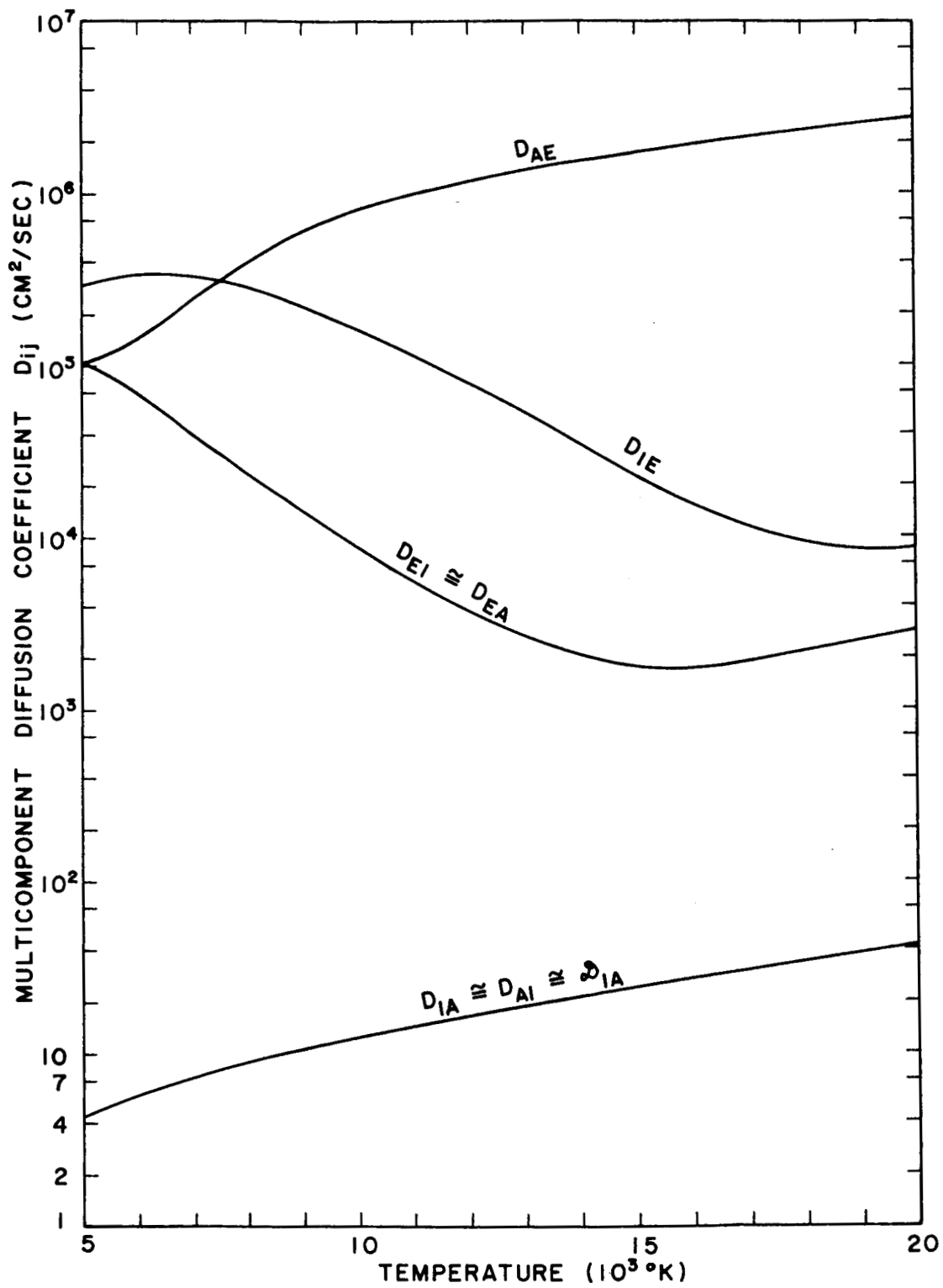


FIG. 18. MULTICOMPONENT DIFFUSION COEFFICIENTS D_{ij} OF EQUILIBRIUM ARGON AT 1 ATM.

$$\lim_{n_E \rightarrow 0} D_{EI} = \lim_{n_E \rightarrow 0} D_{EA} = D_{EA}$$

and

$$\lim_{n_A \rightarrow 0} D_{EI} = \lim_{n_A \rightarrow 0} D_{EA} = D_{EI}$$

(2.17)

In all approximations the calculations showed that it is quite accurate for all degrees of ionization to take $D_{EI} = D_{EA}$. For example, for $p = 100$ mm Hg, a maximum difference of 2% between these coefficients occurs at 87% ionization. Therefore, D_{EI} alone is given in the figures and in Table III. The latter includes a list of the third approximations to D_{AE} , D_{IE} , and D_{EI} at 1000° intervals from 5000 to 20000° K.

The rate of convergence of D_{AE} and D_{EI} (or D_{EA}) at 1 atm is studied in Fig. 19. The rate of convergence is by no means uniform at different temperatures. This feature is to be expected since different intermolecular forces are preponderant at different degrees of ionization. One unexpected result is the reversal of direction of convergence for D_{AE} . Thus at low temperatures D_{AE} increases with higher approximations, while at about 7000° K and above the second approximation is less than the first, and the third is between the two. This behavior, while unusual, has already been encountered in the thermal diffusion ratio of a Lorentzian gas with the Coulomb potential (see I, Table 14).

Because of the very slow rate of convergence of the approximations to D_{AE} and D_{EI} near 5000° K (Fig. 19), it was decided to continue the calculations to even lower temperatures. A limit of 2500° K was determined, mainly by the finite arithmetic of the computer. At low electron and ion densities, we note from (2.16) that

$$[D_{AE}]_1 = [D_{EI}]_1 = [D_{EA}]_1$$

This result is confirmed also by the actual calculations (cf. Fig. 19; note that different scales are used on the abscissa). Figure 20 shows D_{EI} for up to the fourth approximation at pressures of 10 and 760 mm Hg. As mentioned earlier, the average cross sections necessary for

TABLE III. THE ATOM-ELECTRON, ELECTRON-ION AND ION-ELECTRON DIFFUSION COEFFICIENTS (cm^2/sec) FOR EQUILIBRIUM ARGON AT 1, 10, 100, 1900 mm Hg

T ($^{\circ}\text{K}$)	p=1 mm				D _{AE}				D _{EI}				D _{IE}						
	10	100	1900	1	10	100	1900	1	10	100	1900	1	10	100	1900	1	10	100	1900
5000	1.04,8	9.12,6	8.44,5	4.29,4	3.91,7	5.82,6	7.18,5	4.09,4	1.72,8	2.04,7	2.25,6	1.72,8	2.04,7	2.25,6	1.23,5	1.72,8	2.04,7	2.25,6	1.23,5
6000	2.15,8	1.64,7	1.28,6	5.38,4	1.33,7	2.44,6	4.06,5	3.16,4	1.17,8	1.79,7	2.31,6	1.17,8	1.79,7	2.31,6	1.46,5	1.17,8	1.79,7	2.31,6	1.46,5
7000	3.63,8	3.06,7	2.32,6	8.73,4	3.99,6	1.02,6	2.08,5	1.89,4	4.87,7	1.13,7	1.97,6	1.89,4	1.13,7	1.97,6	1.47,5	4.87,7	1.13,7	1.97,6	1.47,5
8000	4.86,8	4.52,7	3.81,6	1.43,5	1.32,6	4.04,5	1.06,5	1.21,4	1.92,7	5.74,6	1.37,6	1.21,4	1.92,7	1.37,6	1.36,5	1.92,7	5.74,6	1.37,6	1.36,5
9000	6.04,8	5.83,7	5.31,6	2.17,5	5.41,5	1.79,5	5.45,4	7.89,3	7.95,6	2.90,6	8.58,5	7.89,3	2.90,6	8.58,5	1.14,5	7.95,6	2.90,6	8.58,5	1.14,5
10000	7.24,8	7.11,7	6.74,6	3.00,5	2.93,5	9.19,4	3.01,4	5.06,3	3.10,6	1.49,6	5.35,5	5.06,3	1.49,6	5.35,5	8.77,4	3.10,6	1.49,6	5.35,5	8.77,4
11000	8.47,8	8.41,7	8.14,6	3.83,5	2.45,5	5.67,4	1.83,4	3.32,3	1.15,6	7.36,5	3.32,5	3.32,3	1.15,6	7.36,5	6.56,4	1.15,6	7.36,5	3.32,5	6.56,4
12000	9.77,8	9.74,7	9.57,6	4.66,5	2.81,5	4.57,4	1.24,4	2.28,3	5.85,5	3.44,5	2.00,5	2.28,3	5.85,5	3.44,5	4.85,4	5.85,5	3.44,5	2.00,5	4.85,4
13000	1.11,9	1.11,8	1.10,7	5.50,5	3.51,5	4.78,4	9.62,3	1.66,3	4.82,5	1.83,5	1.15,5	1.66,3	4.82,5	1.83,5	3.57,4	4.82,5	1.83,5	1.15,5	3.57,4
14000	1.26,9	1.25,8	1.25,7	6.34,5	4.40,5	5.64,4	8.97,3	1.28,3	5.18,5	1.33,5	6.55,4	1.28,3	5.18,5	1.33,5	2.57,4	5.18,5	1.33,5	6.55,4	2.57,4
15000	1.40,9	1.40,8	1.40,7	7.20,5	5.46,5	6.85,4	9.64,3	1.07,3	6.07,5	1.28,5	4.20,4	1.07,3	6.07,5	1.28,5	1.83,4	6.07,5	1.28,5	4.20,4	1.83,4
16000	1.56,9	1.55,8	1.56,7	8.08,5	6.71,5	8.29,4	1.10,4	9.76,2	7.29,5	1.36,5	3.18,4	1.10,4	9.76,2	1.36,5	1.27,4	7.29,5	1.36,5	3.18,4	1.27,4
17000	1.72,9	1.72,8	1.72,7	8.96,5	8.13,5	9.98,4	1.30,4	9.76,2	8.71,5	1.50,5	9.14,3	1.30,4	9.76,2	1.50,5	9.14,3	8.71,5	1.50,5	3.01,4	9.14,3
18000	1.88,9	1.89,8	1.89,7	9.87,5	9.76,5	1.19,5	1.53,4	1.05,3	1.04,6	1.74,5	2.99,4	1.05,3	1.04,6	1.74,5	7.24,3	1.04,6	1.74,5	2.99,4	7.24,3
19000	2.06,9	2.06,8	2.06,7	1.08,6	1.16,6	1.41,5	1.79,4	1.17,3	1.22,6	1.97,5	3.13,4	1.17,3	1.22,6	1.97,5	6.00,3	1.22,6	1.97,5	3.13,4	6.00,3
20000	2.24,9	2.24,8	2.24,7	1.17,6	1.37,6	1.65,5	2.08,4	1.33,3	1.43,6	2.22,5	3.48,4	1.33,3	1.43,6	2.22,5	5.34,3	1.43,6	2.22,5	3.48,4	5.34,3

Notation: 1.04,8 = 1.04×10^8 .

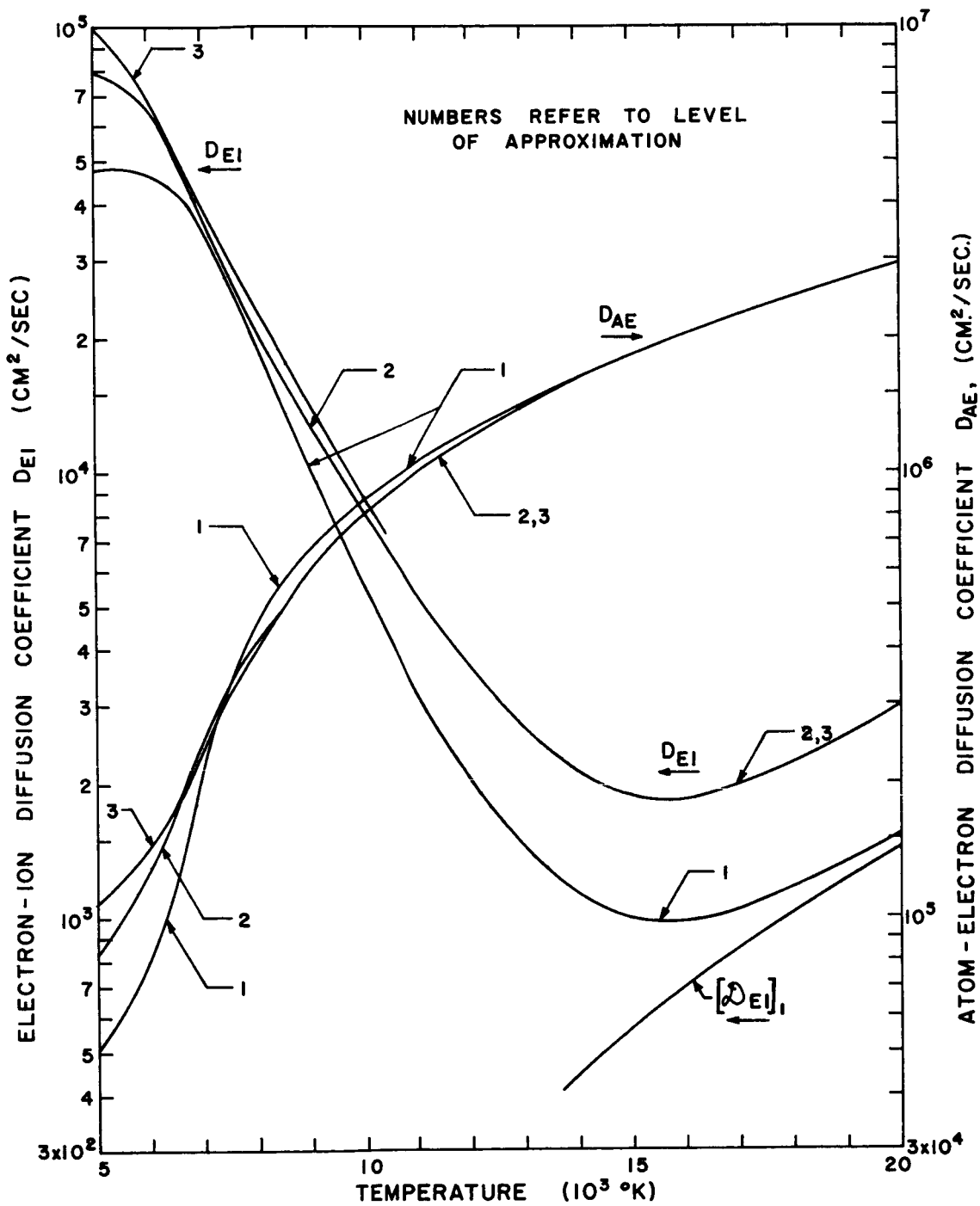


FIG. 19. ELECTRON-ION D_{EI} AND ATOM-ELECTRON D_{AE} DIFFUSION COEFFICIENTS OF EQUILIBRIUM ARGON AT 1 ATM SHOWING RATE OF CONVERGENCE OF APPROXIMATIONS.

the fourth approximation were not available for the exponential potential used for the atom-atom and ion-atom elastic collisions. These cross sections are of minor importance when computing D_{EI} at low temperatures, and so were approximated by

$$\begin{aligned}\bar{Q}^{(2,s)} &= 0.97 \times \bar{Q}^{(2,s-1)} \quad (s = 5,6) \\ \bar{Q}^{(4,4)} &= \bar{Q}^{(2,2)}\end{aligned}\tag{2.18}$$

Note that the cross sections for ℓ odd are not needed for collisions of identical species, and are found from the charge-exchange cross section in the case of the ion-atom pair. Hence only a total of six cross sections must be approximated by (2.18).

One important feature is indicated by Fig. 13, and brought out more strongly in Fig. 20. This is the strong dependence of the slope of the diffusion coefficient curves on the approximation used at the lower temperatures. Thus, at 760 mm, the first approximation to D_{EI} is a monotonic function of T up to about 5250°K where it reaches a maximum and then begins to decrease. The second approximation has a maximum at about 4900°K and then decreases somewhat more rapidly thereafter than the first. In the third approximation the maximum has moved to a slightly lower temperature and a new relative maximum has appeared near 3500°K. This second maximum is confirmed in the fourth approximation and the first maximum has moved to still lower temperatures and become much more pronounced. Because of the complexity of the formulas in the third and fourth approximations, it is difficult to discover the exact source of the maximums in these curves. They probably are caused by the anomalous minimums in the e - A cross sections at low temperatures.

2.3 Comparison of Electrical Conductivity with Experiment

The electrical conductivity appears to be the only transport coefficient of argon which has been measured under conditions in which the state of the gas is reasonably well known. Most of these experiments have been made in the shock tube with the magnetic

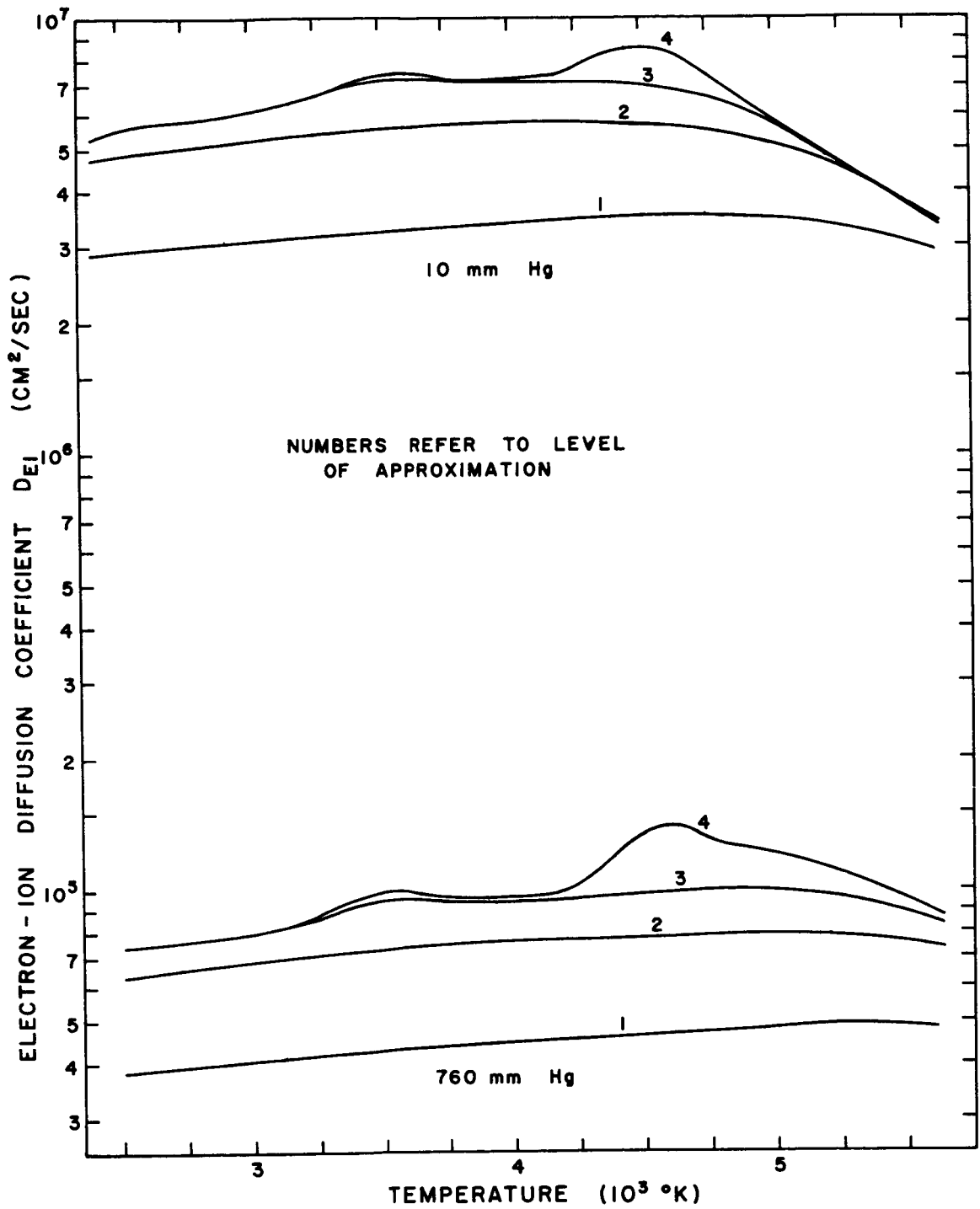


FIG. 20. FIRST FOUR APPROXIMATIONS TO THE ELECTRON-ION DIFFUSION COEFFICIENTS D_{EI} OF EQUILIBRIUM ARGON AT 10 AND 760 mm Hg FOR TEMPERATURES FROM 2500 TO 5500°K.

deflection technique developed by Lin, Resler and Kantrowitz (1955). In one set of data obtained by Pain and Smy (1961), the conductivity was inferred from measurements of the voltages across small electrodes at low currents. The measurements to be considered here were made at initial shock-tube pressures of 1, 10 and 100 mm Hg. Smy and Driver (1963), who worked with an electromagnetic shock tube, report results at lower initial pressures, but the gas apparently does not attain thermodynamic equilibrium at these pressures.

The experimental and theoretical conductivities are shown in Figs. 21-23. The theoretical values were computed with the third approximation. Also shown in Figs. 22-23 is the electrical conductivity as computed from an approximate mean-free-path relation (Lin et al, 1955),

$$\sigma_{\text{MFP}} = \frac{0.532 e^2 n_E}{(m_E kT)^{1/2}} \left[\sum_{i=2}^{\nu} n_i \bar{Q}_{\text{EI}}^{(1,1)} \right]^{-1} \quad (2.19)$$

For the electron-ion encounters, it is necessary to use an average cross section different from the usual one $(3.12)^{\text{I}}$ in order to ensure that σ_{MFP} takes the value of Spitzer and Härm (1953) at full ionization. The cross section so derived is

$$\bar{Q}_{\text{EI}}^{(1,1)} = \frac{0.9 e^4}{(kT)^2} \ln \Lambda \quad (2.20)$$

The usual shock relations were used with the Saha equation (2.10) to determine the state of the gas behind the incident shock. Only below about 10900°K for the initial pressure of 1 mm Hg is the Debye length d greater than the interelectron distance h , so the shielded potential treatment of the charged-particle cross sections is strictly not valid for most of the experimental conditions. Nevertheless the computations were made both with and without the higher order terms and with

$$\Lambda = \max \left(\frac{2d}{b_o}, \frac{2h}{b_o} \right)$$

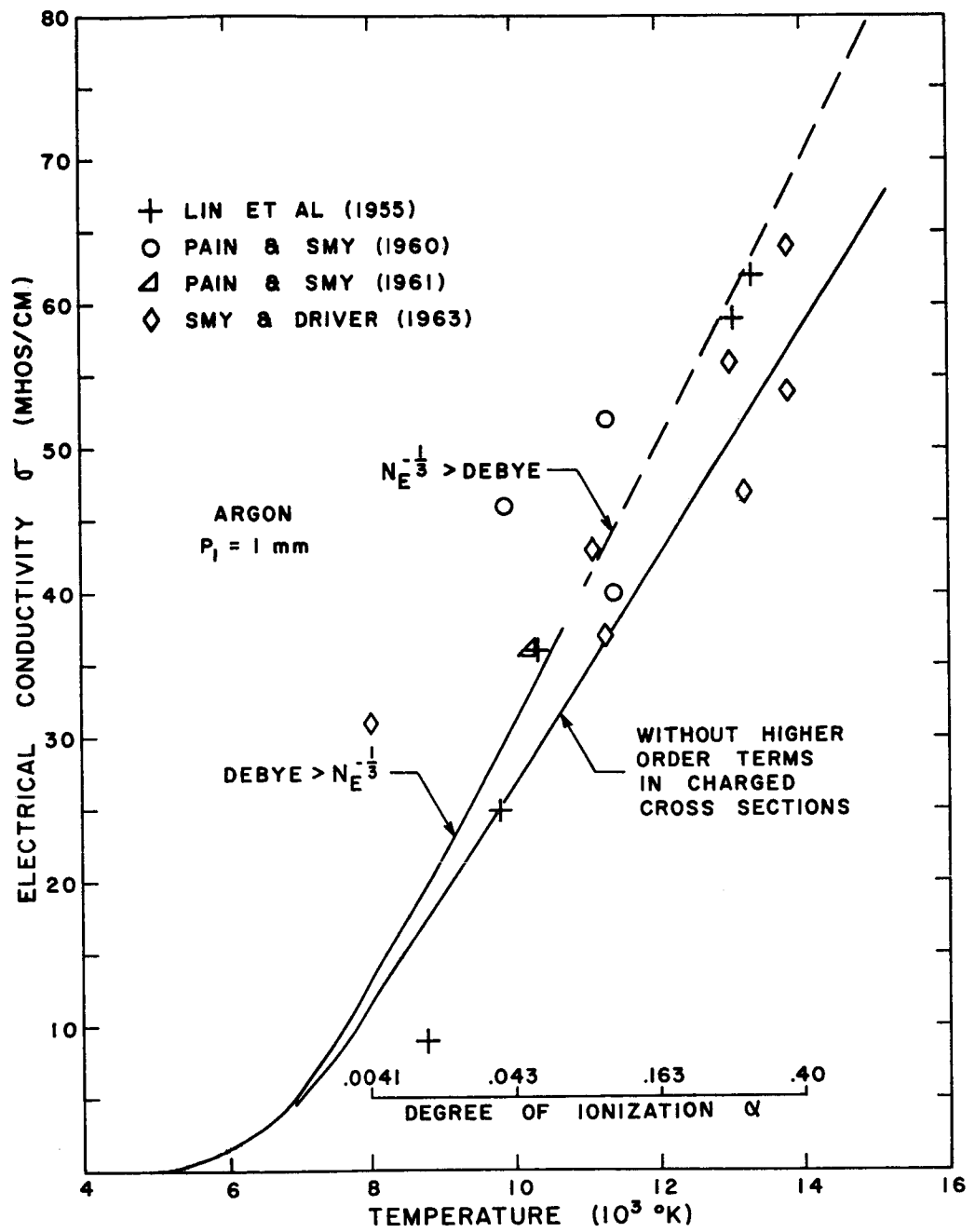


FIG. 21. COMPARISON OF PREDICTED ARGON ELECTRICAL CONDUCTIVITY WITH SHOCK-TUBE MEASUREMENTS AT INITIAL PRESSURES OF 1 mm Hg.

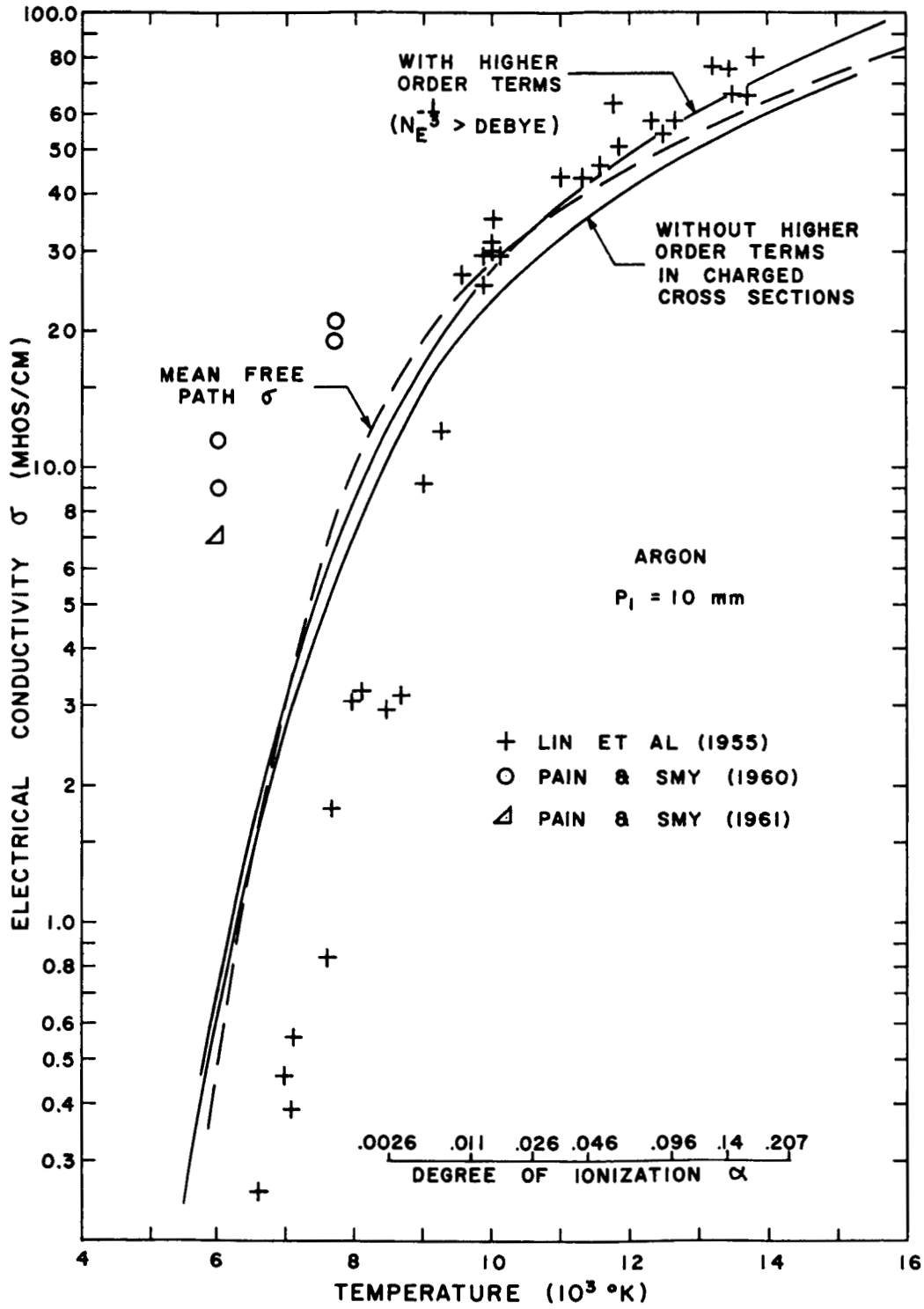


FIG. 22. COMPARISON OF PREDICTED ARGON ELECTRICAL CONDUCTIVITY WITH SHOCK-TUBE MEASUREMENTS AT INITIAL PRESSURES OF 10 mm Hg.

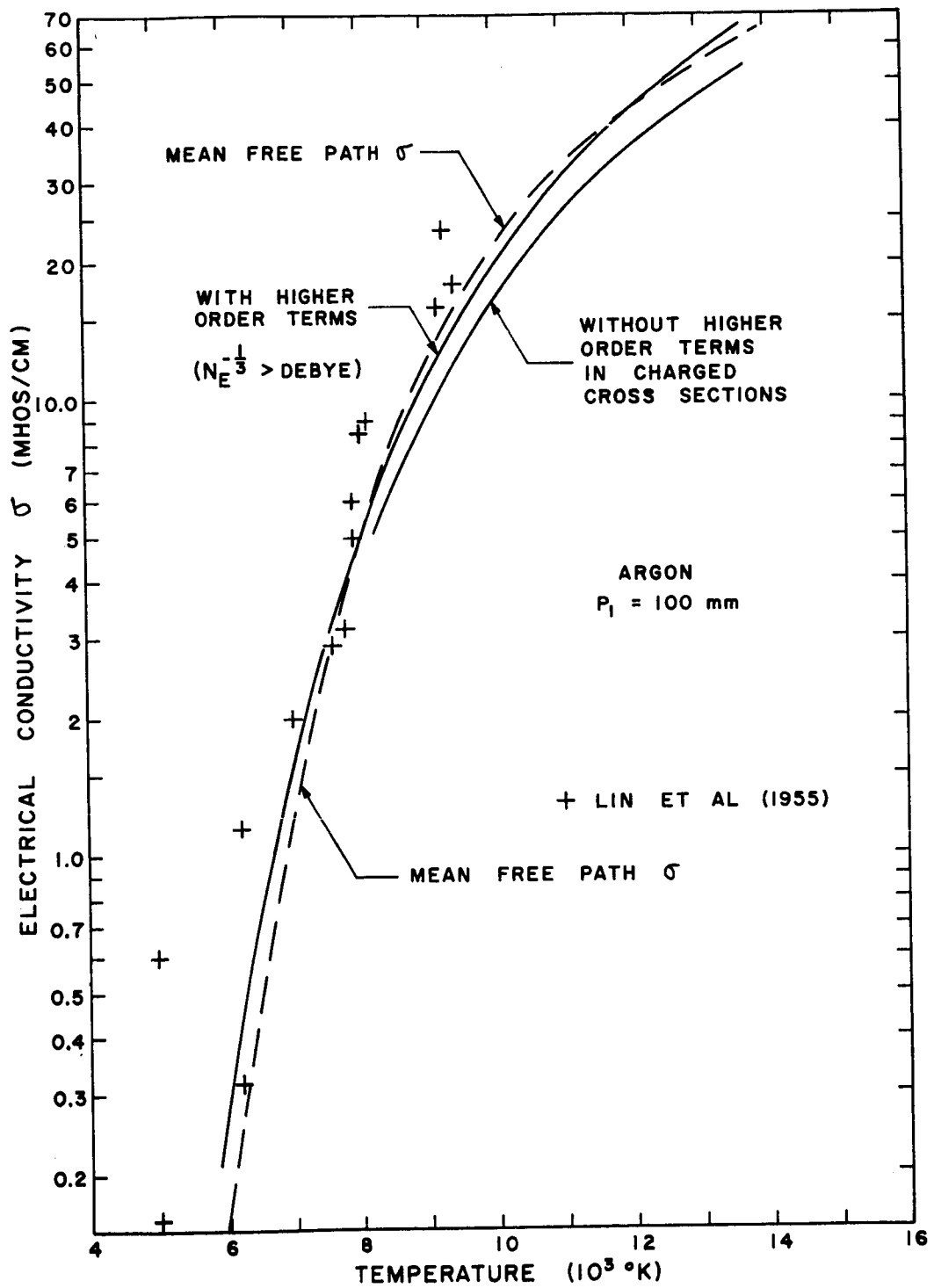


FIG. 23. COMPARISON OF PREDICTED ARGON ELECTRICAL CONDUCTIVITY WITH SHOCK-TUBE MEASUREMENTS AT INITIAL PRESSURES OF 100 mm Hg.

In the figures it appears that the results with the higher order terms give better agreement with the experiments. In the lower temperature measurements of Lin et al (1955), they noted that the conductivity was still rising at the end of the testing time, so the gas had probably not reached equilibrium ionization, which explains why some of these points lie considerably below the curves in Fig. 22. The large discrepancy of some of the points of Pain and Smy (1960, 1961) and Smy and Driver (1963) is unexplained, but might be due to the presence of easily ionized impurities in the test gas.

3. Discussion and Conclusions

We can now compare some of the coefficients computed here with those obtained by other authors. In making these comparisons, we should note that discrepancies can arise from three sources: (1) use of different methods to compute the degree of ionization, (2) the use of different expressions for the coefficients, and (3) different average cross sections.

Errors due to the first source are likely to be important only above about 15000^oK, where the argon atom-atom partition function begins to deviate appreciably from the unexcited value of one. This deviation is often approximated or even entirely neglected. The largest discrepancy due to point (2) would be expected in the thermal conductivity, when the calculations have been carried out with the first or second approximation. But this error can be masked by considerably different choice of average cross sections, even in the charged-particle interactions. Sherman (1963), for example, instead of $\ln \Lambda$ [c.f. (3.12)^I] has used $(1/2) \ln (1 + \Lambda^2)$ with $\Lambda = d/b_o$ and $d^2 = kT/4\pi n_E e^2$ for the $l = s = 1$ cross sections at pressures of 1 atm. In the present case, the interelectron distance h was used instead of d at these pressures, with $\Lambda = 2h/b_o$. Other investigators have approximated the electron-atom cross sections in a variety of ways. Olsen (1959) assumed a constant value, thus completely neglecting the Ramsauer effect. Weber and Tempelmeyer (1964) evidently obtained their average cross sections from the measurements of total cross sections vs energy by setting the average thermal energy ($\approx kT$) equal to the electron energy in scattering experiments. In effect, this method assumes that all electron-atom collisions take place with the average relative speed. But a comparison of Figs. 1 and 2 shows that this method can at best be only a crude approximation to the true variation of $\bar{Q}^{(1,1)}$ with temperature.

The electrical conductivity of argon seems to have been most extensively studied. Olsen (1959) used a mean-free-path expression similar to that given in Section 2.3 to compute σ at 1 atm. His values are considerably above those obtained here (e.g. 97 vs 66 mhos/cm at 15000^oK) or elsewhere. Weber and Tempelmeyer (1964) used two different electron-atom cross sections with the mean-free-path expression (2.19) to obtain

values of σ at 1 atm close to or somewhat above the results of Section 2.2 (e.g. 67 and 87 mhos/cm at 15000°K). Bošnjakovic and Springe (1962) and Pindroh (1962) also report electrical conductivities higher than here (75 and 83 mhos/cm respectively at 15000°K and 1 atm). It should be noted, however, that the inclusion of higher order terms in the charged cross sections increases the electrical conductivity at 100 mm and 15000°K by about 20%. Applying this correction to the value at 1 atm would give a value of 79 mhos/cm, well in the middle of other results.

Cann (1961) and Sherman (1963) have computed the argon viscosity at 1 atm with essentially the first approximation. The values computed by Sherman are considerably higher than those in Fig. 9, probably because of the smaller (constant) ion-atom cross section which he used ($\bar{Q}^{(1,1)} = 78 \text{ \AA}^2$ vs 96 \AA^2 at 15000°K used here). Cann's viscosities are in better agreement but still somewhat high (4.8×10^{-4} vs 4×10^{-4} poise at 16000°K).

The thermal conductivity at 1 atm has been computed in the second approximation by Sherman (1963). Inexplicably, his values at 15000°K (1.03×10^{-5} erg/cm-sec-°K) are considerably above the second approximation in Fig. 13 (0.547×10^5) and not too much below the results for the third approximation (1.22×10^5). Ahtye (1964) also reports a thermal conductivity around 10^5 erg/sec-cm-°K for argon at 15000°K and 10^{-1} atm, but he evidently did not allow for the contribution of thermal diffusion, which would reduce this value by about 40%. Bošnjakovic and Springe (1962) have also reported on calculations with approximate relations due to Maecker and to Schirmer. At 20000°K and 1 atm the former method gives about 3.5×10^5 while the latter gives 2.5×10^5 , in units of erg/sec-cm-°K. Clearly, the latter result is in better agreement with the third approximation as obtained here (2.33×10^5 at 20000°K).

Both Sherman (1963) and Ahtye (1964) have carried out calculations of the diffusion coefficients, although Ahtye only reports values for the thermal diffusion coefficients. A detailed comparison of these coefficients will not be attempted here. It is worthwhile noting the interesting numerical technique used by Sherman to compute the diffusion coefficients as well as the thermal conductivity. Instead of solving the linear equations resulting from the Sonine polynomial expansion and then writing the transport coefficients as the ratio of two determinants (Hirschfelder

et al, 1964; also I), he inverted the matrix of coefficients of the linear equations, and then obtained the transport properties by a simple multiplication of the matrix inverse with a column matrix. This technique results in a large saving of computer time over the method used here whereby one determinant was evaluated for each coefficient (plus one evaluation of the denominator determinant). However, in computation of the third and fourth approximations at low degrees of ionization, the very large disparity in size of some of the matrix elements causes exponent overflow or underflow in the computer when we attempt matrix inversion with the standard programs. It is possible to incorporate features in an inversion program to take care of the possibility of over- or underflow, but it was found easier to do this for the determinant evaluation program. Hence, the expressions involving determinants were used for these computations. For more complicated mixtures, the resultant saving in computer time would make it profitable to investigate further the matrix inversion technique.

We can now turn to a further examination of the calculations presented here, especially with regard to the aims described in the introduction. From the results for the thermal conductivity and for the diffusion coefficients, we can conclude that one should be very careful about assuming that a certain approximation will give adequate transport coefficients when a considerably different force law is operative in the mixture or when a very light species is present. Thus with the Coulomb potential in the fully ionized plasma we must use at least the third approximation to compute the thermal conductivity. The slow convergence carries over into the partially ionized gas, so that there is better than 10% difference between the second and third approximations to these coefficients at 9000°K and 1 atm with a degree of ionization less than 1%! Further, we saw that even the fourth approximation to the electron-ion diffusion coefficient did not appear adequate at very low degrees of ionization. This behavior is doubtless caused by the very different behavior of the dominant electron-atom cross section at lower temperatures. It may be that the expansion in Sonine polynomials is ill-suited for gases with such cross-section behavior.

At the higher degrees of ionization, the inclusion of the next higher order terms in the charged-particle cross sections was found to increase all coefficients by appreciable amounts. In equilibrium argon above about 400 mm Hg this analysis is no longer valid, since the Debye length becomes less than the interelectron distance. When this happens, there are only a few electrons in a Debye sphere, and the concept of shielding by a "cloud" of electrons is lost. However, in the comparison of calculated and experimental electrical conductivities, some evidence was found that the higher order terms for the denser plasmas should be about the same size as those obtained with the shielded potential. The experimental measurements were also compared with calculations made with an approximate mean-free-path expression. Values so computed agreed fairly well with those from the third approximation (as computed without higher order terms in charged cross section); well enough, so that, in view of the large amount of scatter in experimental points, neither could be said to better "predict" the electrical conductivity. However, since the mean-free-path electrical conductivity reduces to a constant times the first approximation to the binary diffusion coefficient at low temperatures, the slow convergence of the latter (see Figs. 19-20) shows that the approximate formula will be seriously in error below about 6000°K.

It is worth reiterating here one conclusion reached in I: that, in spite of the complexity of the expressions, it is possible to routinely carry out computations of the transport properties to the third and even the fourth approximation. The chief stumbling block to such calculations is the lack of knowledge of the average cross sections for all the interactions taking place in the gas. Although we were limited to the third approximation to the thermal conductivity because of the lack of computation of certain average cross sections for the exponential potential, the major need seems to be for further experimental measurements of elastic interactions. Thus, although there have been many measurements of the charge-transfer cross section in argon around 10 eV and above, only one measurement has been discovered in the most important energy range (for gas kinetics at least) around 1 eV. The only absolute

APPENDIX --- GAS-KINETIC CROSS SECTIONS IN TERMS OF PHASE SHIFTS

The method of derivation of Eqs. (2.4a-d) for the gas-kinetic cross sections in terms of the phase shifts η_ℓ will be briefly indicated in this appendix. The differential cross section is given in terms of the phase shifts by

$$\sigma(\chi) = \frac{1}{\kappa^2} \left| \sum_{\ell=0}^{\infty} (2\ell + 1) e^{i\eta_\ell} \sin \eta_\ell P_\ell(z) \right|^2 \quad (\text{A.1})$$

with $\kappa^2 = \mu^2 g^2 / k^2$, $z = \cos \chi$, and $P_\ell(z)$ denoting Legendre polynomials. The object is to evaluate the integrals

$$Q_{(g)}^{(\ell)} = 2\pi \int_0^\pi \sigma(\chi, g) (1 - \cos^\ell \chi) \sin \chi \, d\chi \quad (2.18)^I$$

using this form of the differential cross section. This evaluation is not difficult but is tedious, especially when $\ell = 3$ or 4 . The forms of the result (2.4) for $\ell = 1, 2$ are given in HCB* and are credited there to Kramers, although he apparently did not publish the derivations. To illustrate the method of derivation, the case for $\ell = 1$ will be worked out here. Rewrite (2.18)^I as

$$Q^{(1)} = Q^{\text{TOT}} - \tilde{Q}^{(1)} \quad (\text{A.2})$$

where

$$Q^{\text{TOT}} = 2\pi \int_0^\pi \sigma(\chi) \sin \chi \, d\chi = \frac{4\pi}{\kappa^2} \sum_{\ell=0}^{\infty} (2\ell + 1) \sin^2 \eta_\ell \quad (\text{A.3})$$

is the total cross section. Then,

$$\begin{aligned} \tilde{Q}^{(1)} = & \frac{2\pi}{\kappa^2} \left[\sum_{\ell=0}^{\infty} (2\ell + 1) e^{i\eta_\ell} \sin \eta_\ell \right] \left[\sum_{m=0}^{\infty} (2m + 1) e^{-i\eta_m} \sin \eta_m \right] \\ & \cdot \int_{-1}^1 z P_\ell(z) P_m(z) \, dz \end{aligned} \quad (\text{A.4})$$

* Hirschfelder, Curtiss and Bird (1964)

measurements of the differential cross sections for electron-atom encounters at low energies date from more than thirty years ago (Ramsauer and Kollath, 1932), and have apparently never been quantitatively duplicated. The lack of more recent accurate measurements is more evident when we realize that both Kivel (1959) and O'Malley (1963), whose values of the phase shifts η_ℓ were used to determine $Q^{(\ell)}(g)$ at very low energies, base part or all of their analysis on the Ramsauer-Kollath and earlier measurements.

Using the recursion relation

$$z P_\ell(z) = \frac{\ell}{2\ell+1} P_{\ell-1}(z) + \frac{\ell+1}{2\ell+1} P_{\ell+1}(z) \quad (\text{A.5})$$

and the orthogonality relation

$$\int_{-1}^1 P_\ell(z) P_m(z) dz = \frac{2}{2\ell+1} \delta_{\ell m} \quad (\text{A.6})$$

we see that Eq. (B.2) becomes

$$Q^{(1)} = \frac{4\pi}{\kappa^2} \sum_{\ell=0}^{\infty} \left[(2\ell+1) \sin^2 \eta_\ell - 2(\ell+1) \cos(\eta_\ell - \eta_{\ell+1}) \right. \\ \left. \cdot \sin \eta_{\ell+1} \sin \eta_\ell \right] \quad (\text{A.7})$$

Now expand the expression in brackets and regroup and recombine terms to get

$$Q^{(1)} = \frac{4\pi}{\kappa^2} \sum_{\ell=0}^{\infty} \left[(\ell+1) \sin^2(\eta_\ell - \eta_{\ell+1}) + \ell \sin^2 \eta_\ell \right. \\ \left. - (\ell+1) \sin^2 \eta_{\ell+1} \right]$$

But the last two terms cancel so the final form is

$$Q^{(1)} = \frac{4\pi}{\kappa^2} \sum_{\ell=0}^{\infty} (\ell+1) \sin^2(\eta_\ell - \eta_{\ell+1}) \quad (\text{A.8})$$

The evaluation of the other integrals for $\ell = 2, 3, 4$ follows in much the same way. For the cases $\ell = 3, 4$ the recursion relation (A.5) must be used twice. The results are given in Eqs. (2.4a-d). In the limit $\kappa^2 \rightarrow 0$, $\sin^2 \eta_0 \rightarrow \text{const} \times \kappa^2 = A^2 a_0^2 \kappa^2$ (say), and the other phases vanish as κ^4 or a higher power of κ . In this limit, then,

$$Q^{\text{TOT}} \sim 4\pi A a_0^2$$

$$Q^{(1)} \sim Q^{\text{TOT}}$$

$$Q^{(2)} \sim \frac{2}{3} Q^{\text{TOT}}$$

(A.9)

$$Q^{(3)} \sim Q^{\text{TOT}}$$

$$Q^{(4)} \sim \frac{252}{315} Q^{\text{TOT}}$$

BIBLIOGRAPHY

- Ahtye, W. F. (1964), "A Critical Evaluation of Methods for Calculating Transport Coefficients of a Partially Ionized Gas," in Proceedings of the 1964 Heat Transfer and Fluid Mechanics Institute, Stanford University Press.
- Amdur, I. and Mason, E. A. (1958), "Properties of Gases at Very High Temperatures," *Phys. Fluids*, 1, 370.
- Biondi, M. A. and Chanin, Lm M. (1952), "Temperature Dependence of Ion Mobilities in He, Ne and A," *Phys. Rev.*, 106, 473.
- Bošnjakovic, F. and Springe, W. (1962), "Electrical and Thermal Conductivity of Argon Plasma," in Progress in International Research on Thermodynamic and Transport Properties, ASME, N.Y.
- Brokaw, R. S. (1964), "Approximate Formulas for Viscosity and Thermal Conductivity of Gas Mixtures," NASA TN D-2502.
- Cann, G. L. (1961), "Energy Transfer Processes in a Partially Ionized Gas," Hypersonic Research Project Memo. No. 61, Guggenheim Aeronautical Laboratory, Cal. Inst. Technology.
- Chapman, S. and Cowling, T. G. (1958), "The Mathematical Theory of Non-Uniform Gases," Cambridge University Press.
- Cloney, R. D., Mason, E. A. and Vanderslice, J. T. (1962), "Binding Energy of A_2^+ from Ion Scattering Data," *J. Chem. Phys.*, 36, 1103.
- Cramer, W. H. (1959), "Elastic and Inelastic Scattering of Low Velocity Ions: Ne^+ in A, A^+ in Ne and A^+ in A," *J. Chem. Phys.*, 30, 641.
- Dalgarno, A. (1958), "The Mobilities of Ions in Their Parent Gases," *Phil. Trans. Roy. Soc. London*, A250, 426.
- de Voto, R. S. (1964), "Transport Properties of Partially Ionized Monatomic Gases," SUDAER No. 207, Dept. of Aeronautics and Astronautics, Stanford University.
- Drellishak, K. S., Knopp, C. F. and Cambel, A. B. (1963), "Partition Functions and Thermodynamic Properties of Argon Plasma," *Phys. Fluids*, 6, 1280.
- Fay, J. A. (1962), "Hypersonic Heat Transfer in the Air Laminar Boundary Layer," AMP 71, Avco Everett Research Lab., Everett, Mass.
- Firsov, O. B. (1951), *Zh. Eksperim. i Teor. Fiz.*, 21, 1001.
- Gilbody, H. B. and Hasted, J. B. (1957), "Anomalies in the Adiabatic Interpretation of Charge Transfer Collisions," *Proc. Roy. Soc. London*, A238, 334.

- Hirschfelder, J. O., Curtiss, C. F. and Bird, R. B. (1964), "Molecular Theory of Gases and Liquids," John Wiley & Sons, New York.
- Kivel, B. (1959), "Elastic Scattering of Low Energy Electrons by Argon," Phys. Rev., 116, 926; also Research Note 129, AVCO Everett Research Lab., Everett, Mass.
- Kushnir, R. M., Palyukh, B. M. and Sena, L. A. (1959), "Investigations of Resonance Charge Exchange in Monatomic Gases and Metal Vapors," Bull. Acad. Sci. USSR, Phys. Ser., 23, 995.
- Liboff, R. L. (1959), "Transport Coefficients Using the Shielded Coulomb Potential," Phys. Fluids, 2, 40.
- Lin, S. C., Resler, E. L. and Kantrowitz, A. (1955), "Electrical Conductivity of Highly Ionized Argon Produced by Shock Waves," J. Appl. Phys., 26, 95.
- Lindholm, E. (1960), "Ionization and Dissociation of H₂, N₂ and CO in Charge Exchange Collisions with Positive Ions," Arkiv Fysik, 18, 219.
- Mason, E. A., Vanderslice, J. T. and Yos, J. M. (1959), "Transport Properties of High Temperature Multicomponent Gas Mixtures," Phys. Fluids, 2, 688.
- Monchick, L. (1959), "Collision Integrals for the Exponential Repulsive Potential," Phys. Fluids, 2, 695.
- O'Malley, T. F. (1963), "Extrapolation of Electron-Rare Gas Atom Cross Sections to Zero Energy," Phys. Rev., 130, 1020.
- Olsen, H. N. (1959), "Thermal and Electrical Properties of an Argon Plasma," Phys. Fluids, 2, 614.
- Pain, H. J. and Smy, P. R. (1960), "The Electrical Conductivity of Shock Heated Argon," J. Fluid Mech., 9, 390.
- Pain, H. J. and Smy, P. R. (1961), "Experiments on Power Generation from a Moving Plasma," J. Fluid Mech., 10, 51.
- Pindroh, A. L. (1962), "Transport and Electrical Properties of the Inert Gases," D2-22422, Boeing Company. Argon Properties Quoted in D2-11238.
- Ramsauer, C. and Kollath, R. (1932), "Die Winkelverteilung bei der Streuung langsamer Elektronen an Gasmolekülen III. Fortsetzung und Schluss," Ann. Physik, 12, 837.
- Sherman, M. P. (1963), "Calculation of Transport Properties - Mixtures of Helium and Partly-Ionized Argon," Princeton University, Aero. Engineering Laboratory Report No. 673.

Smy, P.R. and Driver, H.S. (1963), "Electrical Conductivity of Low Pressure Shock Ionized Argon," J. Fluid Mech., 17, 182.

Spitzer, L. and Härm, R. (1953), "Transport Phenomena in a Completely Ionized Gas," Phys. Rev., 89, 977.

Weber, R. E. and Tempelmeyer, K. E. (1964), "Calculation of the D-C Electrical Conductivity of Equilibrium Nitrogen and Argon Plasma with and without Alkali Metal Seed," Arnold Engineering Development Center, Report No. AEDC-TDR-64-119.

Westin, S. (1946), "Investigations on the Elastic Scattering of Slow Electron in Helium, Neon, and Argon," Det Kgl. Norske Videnskabers Selskabs Skrifter, Nr. 2, F. Bruns Bokhandel, Trondheim.

Ziegler, B. (1953), "Der Wirkungsquerschnitt seher langsamer Ionen," Z. Physik, 136, 108.